CLEAN WATER

WATER POLLUTION CONTROL RESEARCH SERIES ● 16020 FQT 12/70

Fluid Product Pipeline Leak Detection From Airborne Platforms

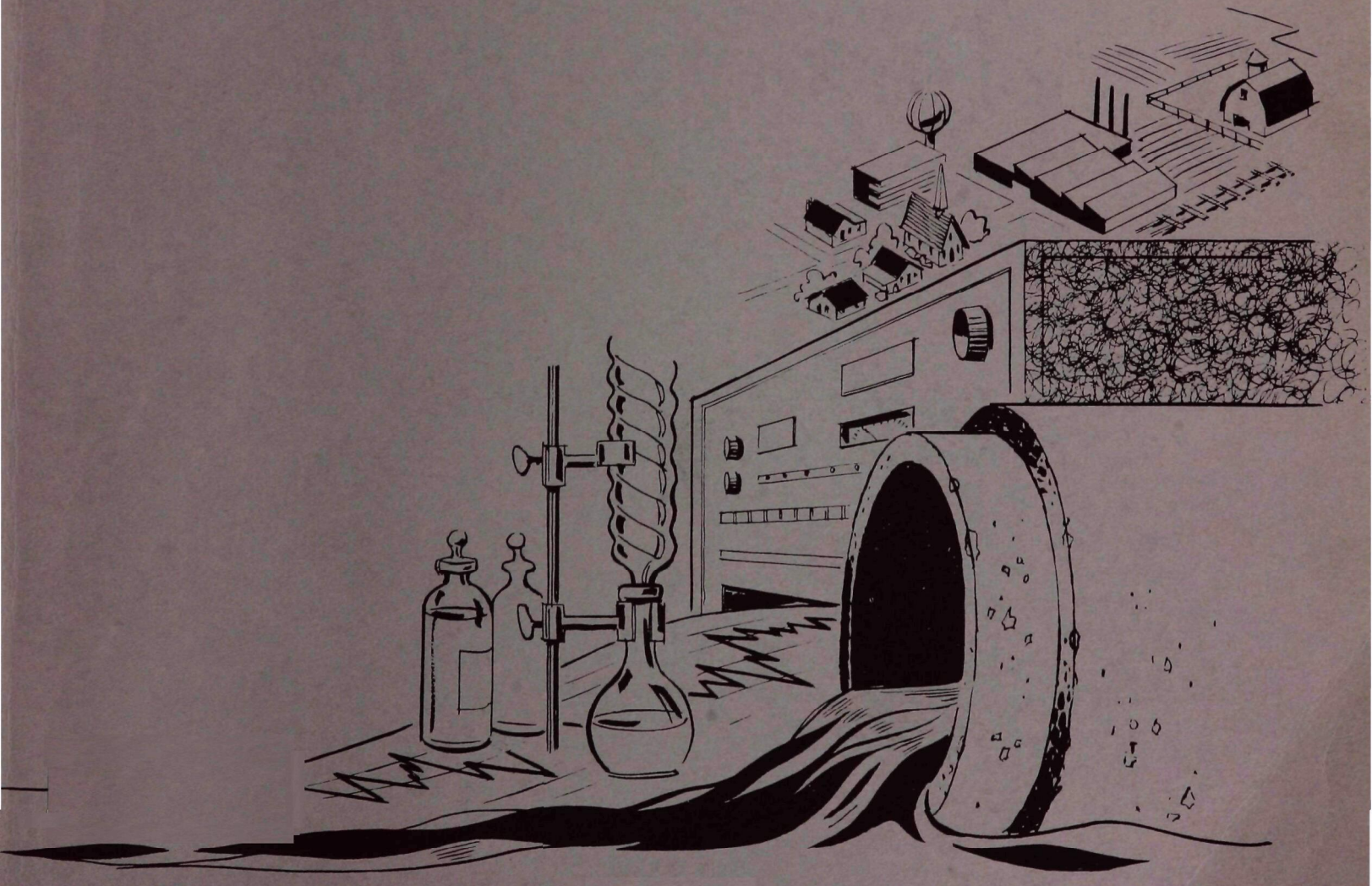

U.S. ENVIRONMENTAL PROTECTION AGENCY

WATER POLLUTION CONTROL RESEARCH SERIES

The Water Pollution Control Research Series describes the results and progress in the control and abatement of pollution in our Nation's waters. They provide a central source of information on the research, development and demonstration activities in the Environmental Protection Agency, through inhouse research and grants and contracts with Federal, State, and local agencies, research institutions, and industrial organizations.

Inquiries pertaining to Water Pollution Control Research Reports should be directed to the Chief, Publications Branch (Water), Research Information Division, R&M, Environmental Protection Agency, Washington, D.C. 20460.

FLUID PRODUCT PIPELINE LEAK DETECTION FROM AIRBORNE PLATFORMS

by

Resources Technology Corporation
1275 Space Park Drive
Houston, Texas 77058

for the

ENVIRONMENTAL PROTECTION AGENCY

Program #16020 FQT
December, 1970

For sale by the Superintendent of Documents, U.S. Government Printing Office, Washington, D.C. 20402 - Price $1.00

EPA Review Notice

This report has been reviewed by the Environmental Protection Agency and approved for publication. Approval does not signify that the contents necessarily reflect the views and policies of the Environmental Protection Agency nor does mention of trade names or commercial products constitute endorsement or recommendation for use.

ABSTRACT

A computer simulation program in conjunction with an instrument systems analysis program lead to the conclusion that microwave radiometry working in concert with thermal infrared systems could detect petroleum product pipeline leaks. The utilization of these systems from an airborne platform would result in a low false alarm rate and a high probability of leak detection. A demonstration experiment was designed to test the simulation program. This demonstration was carried out in west Texas along three different pipeline sections with eighteen individual leak circumstances.

Three ground crews, one for each pipeline section, marked the sections of pipeline and each individual leak as well as gathering ground data consisting of oil saturation, soil moisture, and thermal temperatures at both the surface and subsurface to ten inches.

All data, airborne and ground, was reduced, correlated and analyzed to demonstrate remote sensor capabilities. It was found that the apparent microwave (13.7 GHz) temperature of a leak increases significantly compared to surface material containing no oil. Also, a soil containing oil caused a decrease in polarization contrast. Thermal infrared showed a warm area surrounded by a cool halo. When these circumstances all occurred together a leak was identified, proving the correctness of the original computer simulations.

This report was submitted in fulfillment of project 16020 FQT under the sponsorship of the Water Quality Office, Environmental Protection Agency.

CONTENTS

Section		Page
I	Summary and Introduction	1
II	Conclusions and Recommendations	7
III	Program History and Development	9
IV	Field Measurements Program	31
V	Data Correlation and Reduction	47
VI	Data Analysis and Interpretation	51
VII	Problem Areas and Solutions	67
VIII	Appendix A - Radiometer Data Reduction Procedures	75

FIGURES

No.		Page
1	Microwave Temperature Variations as a Function of Changing Moisture Content, 3.0 GHz	14
2	Microwave Temperature Variations as a Function of Changing Moisture and Oil Content, 0.3 GHz	17
3	Microwave Temperature Variations as a Function of Changing Moisture and Oil Content, 3.0 GHz	18
4	Microwave Temperature Variations as a Function of Changing Moisture and Oil Content, 10 GHz	19
5	Microwave Temperature Variations as a Function of Changing Moisture and Oil Content, 0.3 GHz	20
6	Microwave Temperature Variations as a Function of Changing Moisture and Oil Content, 3.0 GHz	21
7	Microwave Temperature Variations as a Function of Changing Moisture and Oil Content, 10 GHz	22
8	Polarization Contrast, ΔT_p, for Soil Containing Oil and Moisture at 0.3 GHz	23
9	Polarization Contrast, ΔT_p, for Soil Containing Oil and Moisture at 3.0 GHz	25
10	Polarization Contrast, ΔT_p, for Soil Containing Oil and Moisture at 10 GHz	26
11	Computer Simulation of Pipeline Leak Detection	28
12	End of Flight Line Markers	38
13	Aluminum Panel Electromagnetic Markers	38

FIGURES (continued)

No.		Page
14	Leak Site Identification Markers	39
15	Schematic Diagram of a Test Site	39
16	Site 1, West of Crane, Crane County, Texas	43
17	Site 2, Southeast of Wink, Winkler County, Texas	44
18	Site 3, East of Wink, Winkler County, Texas	45
19	Multisensor Data Correlation, Site 1	53
20	Multisensor Data Correlation, Site 2	58
21	Multisensor Data Correlation, Site 3	66
22	Profile Offset Due to Wind	68
23	Profile Ground Track, Site 1	70
24	Profile Ground Track, Site 2	71
25	Profile Ground Track, Site 3	72
26	Schematic of Incredata Tape	76
27	Definitions of Roll, Pitch and Yaw	80
28	Strip Chart Recording of Serial Digital and Audio Channels	85
29	Strip Chart Recording Used for Timing	87

TABLES

No.		Page
1	Dielectric Constants of Soil and Water	16
2	Computed Radiometric Temperature Differentials	27
3	Surface Measurements, Site No. 1 (Night)	54
4	Surface Measurements, Site No. 1 (Day)	55
5	Surface Measurements, Site No. 2 (Night)	61
6	Surface Measurements, Site No. 2 (Day)	62
7	Incredata Digital Tape Print-Out	82
8	Incredata Digital Tape Print-Out	83

SECTION I

FLUID PRODUCT PIPELINE LEAK DETECTION FROM AIRBORNE PLATFORMS

SUMMARY AND INTRODUCTION

Initial research indicates that oil spilled from leaks in land traversing pipelines is much more common than ordinarily anticipated. In fact the quantities of oil that infiltrate continental soils from leaks in trunk and gathering lines may equal that spilled on the oceans. In general it is the lack of visible mobility that has been a deterent to identifying pipeline leaks as a form of continental pollution. However, these spills represent a source of pollution to all continental water supplies including surface run-off, acquifers and general ground water systems. In the process of examining various pipeline sections to select proper sites for the conduct of this program, oil leaks and hydrocarbon surface trails were found which flowed into local streams, saturated ground next to city water supply wells and potentially contaminated near surface gravels normally utilized for water supply. In addition large areas contaminated by hydrocarbon saturation caused the demise of local vegetation and for all practical purposes made local areas unfit for any use. The areal extent of land affected by pipeline leaks has not been determined. However, the ubiquity of pipeline leaks indicate the numbers would be surprisingly large.

However, the objective of this program is not to analyze pipeline leaks as a contaminate, but to test airborne sensors which may detect oil leaks early in their history. As a precursor to the reported survey program a systems analysis was performed to determine which remote sensors would have the highest potential of detecting pipeline leaks from an airborne platform. It was determined that a combination of microwave radiometry supported by infrared thermal imagery offered the greatest potential. Computer models of pipeline leak circumstances were generated to further test the feasibility of these systems prior to conduct of the actual survey. Both the systems analysis and the computer models indicated potential success and actual field testing was initiated. The field tests were posivive for airborne detection of leaks in the environment tested. However, problem areas in the utilization of such systems were identified which require further study before operational systems can be defined.

Systems Analysis

The greatest potential for pipeline leak detection exists using electromagnetic sensors. Unfortunately there are no all-spectrum detection devices. Therefore, the electromagnetic spectrum was separated into spectral regions based on instrument types. The following criteria were used to arrive at a final selection:

- The system should have day/night capabilities.
- Detection should not be limited by weather conditions.
- The system should "penetrate" the surface to detect the presence of subsurface oil.
- The effects of rough ground should be minimized.
- Detection through foliage is highly desirable.
- The system should not interfere with local communications.
- The system must be light weight; capable of instal lation on a light aircraft.
- Data reduction and analysis should be simple, inexpensive and accomplished rapidly.

These criteria were most nearly fulfilled by passive microwave radiometers and thermal infrared imaging systems.

The Simulated Models

The basic premise is that the addition of oil to a soil would cause a change in the dielectric constant of the soil. The change in dielectric constant in turn results in a change in electromagnetic emission characteristics. If these changes are large enough then oil leaks should be detectable.

The calculations of the effects of adding oil to a soil is not a simple task. First, not only are soil and oil involved but the moisture content (water) in the soil must also be considered. This means that dielectric mixing formulas involving three dielectrics must be considered.

The approach first developed a data set for soil containing water only. This was followed by a data set involving only

soil and oil. These were then combined to determine a data set for oil/water/soil systems.

These models showed that in all circumstances, using various percentages of each constituent, that the addition of oil caused perturbations that should be detectable. The emissivity is increased such that the detected apparent temperature of the leak area is increased. Also, the differential emissivity for the horizontal and vertical polarized energy is decreased, resulting in a smaller differential between apparent temperatures detected for the horizontal and vertical polarized energy components.

Therefore, the prediction models indicate two mechanisms for identifying petroleum product pipeline leaks: An increase in the detected apparent temperature contrast; and a reduction in polarization contrast. When both of these are combined in the analysis phase a high probability of detection with a low false alarm rate results.

The Field Survey

Three sections of pipeline in west Texas were selected for the demonstration flights. Each section was approximately two miles long and had four to seven identifiable leaks at each site.

Ground survey teams (3) marked the beginning and end of each of the three pipeline sections such that positive identification could be made by the pilot. Also each field team gathered ground data which include ground temperature, ground moisture content, hydrocarbon saturation, and general wind speed and direction. These data were used in the analysis phase.

Two aircraft were utilized to obtain data, one for high altitudes (2,000' above ground) and one low altitude (500' above ground). The instrumentation in the low altitude aircraft proved faulty so that only the high altitude platform was used, and the altitude was reduced to 1,000 feet above ground. No further problems were encountered in the field program and the following simulaneous data were obtained for each of the three sites:

- Color Photography - Ektrachrome 2448
- RS-14 Infrared Imagery 9-14 microns
- Black and White Photography - Plus X 2402
- Black and White Infrared Photography - 2424

- Color Infrared Photography - 8443
- Microwave Radiometric Profiles - 13.7 GHz

Each site was flown during the day (all sensors) and during the night (infrared and microwave only).

There were no problems, other than the failure of the low altitude aircraft, encountered in the field operation and all data gathered were valid and ready for data processing and analysis.

Data Processing

All photographically recorded data were processed using standard development and printing techniques. Correlation between various photographic and imagery sensors was easily accomplished by matching image characters such as roads, houses, oil wells and vegetation groupings. Scale factors were determined by two techniques: measuring the film dimensions of known ground targets, whose actual dimensions were known; and using camera focal lengths and aircraft altitude formulas. These scale determination functions were well within error budgets and correspondance was excellent.

The correlation between microwave data and imagery data was accomplished using two systems. The prime technique employed aluminum foil panels on the ground. These caused cold anomalies on both IR imagery and microwave profiles. These panels in turn were identified on the photography and start and stop points were identified for all sensors simultaneously. The second technique was based on time and internally generated 400 Hz signals. At the beginning and end of each data run 400 Hz signals were impressed on the magnetic recording tapes. In this manner all sensors could be simultaneously related to start and stop points. Since the microwave radiometer was viewing aft at an angle of 45^{o}, it was necessary to slide the profiles forward an amount equivalent to the altitude of the aircraft. Also, because the microwave system produces only a profile, it was necessary to compensate for roll, pitch and yaw of the aircraft. These parameters were recorded inflight by an Incredata system and geometric corrections were made such that a profile was indeed identified as to actual ground intercept position. All microwave data were corrected by computer programs generated for a CDC-6600 computer system and coded in FORTRAN IV. The computer output was played into a Cal-Comp plotter and the corrected profiles plotted for use in data analysis.

Data Analysis

All the obtained data were mounted on data boards (one for each site) such that point-to-point correspondence of data was established. All data were then examined to determine the response of each sensor.

The basic premise derived from the computer modeling program was found to be correct. That is, the apparent microwave temperature did increase and the polarization contrast did decrease when an oil leak was encountered.

The infrared imagery was also valuable in detecting leak zones. The centers of active leak areas appeared hot, surrounded by cool anomalies associated with hydrocarbon trails. It appears that fresh oil in a soil appears warm and dead oil (old) appears cool. However, there is a "greenhouse" effect which causes an increase in subsurface water content beneath the spill. This may have an effect on detection capabilities which increase the probability of leak identification. Certainly it is something that should be considered.

All leaks were visible and detectable with color photography except two leaks at site 2. These were identified as potential leaks by microwave radiometry and the color photographs were re-examined for surface staining indicative of a leak. Staining was found at one microwave anomaly and very slight traces, which may be leak staining at the other. Neither of these areas would have been called "leaks" without microwave identification. Field sampling of these potential leaks has not been accomplished and positive identification as leaks has some uncertainty. However, the slight surface staining strongly suggests a leak circumstance.

Black and white photography and black and white photographic infrared and color infrared images were very erratic in being useful for leak detection. Some of the larger leaks were quite obvious on the images, but some were marginal and many of the smaller leak "scars" were undetectable with these systems.

Identification and detection of oil leak zones using 13.7 GHz microwave profiles along the surveyed pipeline sections were positive when both the apparent temperature raise and polarization decrease were used together. Either one separately were of little value and had high false alarm rates. When used together the false alarm rate was nearly zero for those leak zones encountered by the horizontal and vertical beams. However, not all leaks were encountered by both beams and a total analysis was not possible. This was due to the inability to fly exactly the same flight line twice.

Problem Areas

Three major problem areas developed in performing analysis of the obtained data. These were errors in pilot judgement, aircraft dynamics and polarization differential.

Pilot judgement was the dominant problem. When using profiling instruments that require flying the exact same track several times, proper visual alignment is critical. This is especially true if the instruments view the ground from some angle other than nadir. Winds blowing at angles to the flight path force the pilot to "crab" the aircraft into the wind in order to fly a straight line. This means that instruments viewing at some angle are not tracking along the path desired.

Aircraft dynamics such as pitch, roll, yaw and velocity changes cause deviations from the desired ground track. These deviations can be corrected for by recording the dynamic deviation and geometrically determining where the true ground intercept occurred. However, this only tells if the proper target was encountered or not. If it was missed, after the fact knowledge does not make the information recoverable.

The computer simulations program, which initiated this project, predicted a decrease in polarization contrast ($T_V - T_H$). The actual polarization differential was very nearly zero, that is $T_V = T_H$, which was not predicted. Obviously the model is not totally adequate or the acquired data included circumstances which were not totally due to leak characteristics.

The solutions to these problems are relatively simple, but require instrumentation that is difficult to obtain. Both the pilot judgement and aircraft dynamics problems can be solved by using multibeam or imaging systems. This would alleviate the problem of very accurate flying. The polarization problem can be solved by using microwave systems which have simultaneous dual polarization data acquisition capabilities. These systems are presently available and will be used on future projects.

SECTION II

CONCLUSIONS AND RECOMMENDATIONS

The total project was successful in proving that microwave and infrared systems are indeed valuable for detecting the delineating leaks in petroleum product trunk lines, especially under the environmental circumstances encountered. Basically the computer models were correct and the electromagnetic characteristics of soils are changed by oil to the extent that existing instrumentation can be used to detect, delineate and map leaks. The "all-weather" day/night capabilities of microwave systems has already been proven. Therefore, the potential of using microwave systems as a leak detection system in areas of inclimate weather is real.

It is highly recommended that the program, as started, be continued to include other environmental type areas. The ability to operate in forested areas, swamps and agricultural areas has not been established. Experiments to test these environment types should be conducted to bring this entire demonstration program to a proper and logical conclusion.

It is also recommended that the suggested solutions to the problem areas as outlined be incorporated in the next set of experiments.

An expansion of the program to test water quality in areas where leaks have occurred close to local or regional water supplies is also in order. The fact that pipeline leaks are much more prevalent than normally thought, leads to the conclusion that water quality may be affected much more than present considerations anticipate.

SECTION III

PROGRAM HISTORY AND DEVELOPMENT

The need to "clean up America" has been brought forceably to the attention of the American public and government, simply because pollution of the air and natural waters became so apparent that it could no longer be ignored. The American public is looking to the State and Federal Governments to protect them from further pollution and to reduce pollution that presently exists.

This report is concerned with a type of pollution that is not generally considered because it is invisible in most cases and does not irritate the eyes or affect the respiratory system. This is the pollution of ground water and aquifers by leaks in oil product pipelines. Oil from product pipelines migrating into soil is not only a potential contaminant of ground water supplies, but once subjected to saturation or even mild contamination by oil, an area loses its agricultural potential and all vegetation in the area dies very rapidly. Furthermore, once soil is contaminated by oil, it is almost impossible to flush it out.

Thousands of miles of product pipelines crisscross the United States carrying almost every conceivable kind of bulk fluid. The total line-miles crossing Federal lands represent a major part of all these pipelines. Aircraft are used to examine pipeline right-of-ways on a routine basis. However, examination is by visual observation, generally only the pilot. As a result leaks which are so gross that they saturate the surrounding areas to the surface are the only ones detected.

As pipelines age, they become more and more subject to leakage. Many major lines are decades old making continuous surveillance a must, if only from a hazard point of view.

RESOURCES TECHNOLOGY CORPORATION completed a study to determine the feasibility of using modern electromagnetic sensors for detecting subsurface pipeline leaks. The study indicates that relatively simple instrumentation may be used on light aircraft to detect pipeline leaks that are not readily apparent

Airborne electromagnetic radiation sensors were examined in detail to determine which sensors had the highest probability of achieving the set goals.

The natural development of instruments for remote sensing has been an extension of human functions, primarily to increase detectability. Optics aid the visible senses through magnification of objects, and cameras were developed to permanently

record those objects that could be visibly detected. "Seeing" capabilities have been extended by orders of magnitude by using many different devices. The spectra of human sight has even been extended into the infrared and ultraviolet by clever detection and display systems.

During and since World War II, extensive investigations have been undertaken to extend the ability to "see", detect, and discriminate objects in the microwave portion of the electromagnetic spectrum. The primary objective was to develop systems which could "see" for long distances, day and night, and penetrate heavy weather conditions. The outcome of these efforts was the development of RADAR.

In general, there are two modes of operation for these new geophysical sensors, active and passive. In the active mode electromagnetic energy is transmitted from a source and reflected energy is received, registered, and analyzed. In the passive mode naturally emitted electromagnetic energy is received, detected, and displayed for analysis.

It has been firmly established by a number of studies sponsored by the Federal Government and private industry, that energy in the microwave region of the electromagnetic spectrum (from 10^9 CPS to 10^{11} CPS) has some capability of penetrating dense dielectric materials such as soil, rock and oil. Also these systems operate efficiently during day or night and during inclimate weather conditions. Since operations are not dependent on time of day or weather conditions, airborne operations of passive microwave systems are extremely flexible and useful.

Existing empirical data on soils and earth surface materials, combined with available data on petroleum products were utilized to determine the practical capabilities of detecting leaks in petroleum product pipelines using passive microwave radiometers and known data analysis techniques. Initial models and simulations established that microwave radiometry could be used from an airborne platform to detect pipeline leaks, since it appears that the radiometric anomalies for oil added to various soils are large.

A field measurements program was designed and carried out to test the developed models. This report covers both aspects, modeling and the obtained field data.

Statement of the Problem

Leakage of underground pipes which transport refinery products or crude oil needs to be detected rapidly if breakage occurs,

not only to protect the owner of the pipeline and the public, but to prevent long term contamination of ground water supplies. Testing the application of remote sensing methods to the solution of the problem appears appropriate.

Electromagnetic Sensors

Electromagnetic radiation is energy produced by the oscillations of charged atomic and molecular particles. It is a continuum function in that particle vibration occurs at all possible vibrational frequencies. This radiation is characterized chiefly by frequency (wavelength), intensity, polarization and phase. Radiation can only react or change when photons interact with matter. Electromagnetic energy in free space does not interact with electromagnetic energy from the same or different sources. This lack of interaction in free space is the essential ingredient utilized by the communications industry and allows electromagnetic sensor systems such as infrared, photography, radar and microwave radiometry, to be used as remote sensor systems.

Unfortunately, there are no all-spectrum detection devices or mechanisms, so the electromagnetic spectrum has been separated into various spectral regions based primarily on instrument type. Because of this, the requirements for a specific problem area, such as the detection of pipeline leaks, must be analyzed to determine which instrumentation is most suitable. This analysis for pipeline leak detection was performed using the following criteria:

- The systems utilized should have day/night capabilities with little change in signal characteristics. The detection of pipeline leaks should not be limited in time.
- Detection of pipeline leaks should not be limited by weather conditions. Fog, light rain, cloud conditions or snow should not prevent detection of leak areas.
- The selected system should have penetration capabilities or receive signals from sufficient depths that primary and secondary subsurface anomalies can be sensed.
- Surface features such as rough ground should have a minimum effect on detection capabilities.
- Detection through foliage is highly desirable.

- The system should be passive so that interferences with local FM, TV, and other communications systems will not present problems. Also frequency of operation should be separated from weather and aircraft radar operating frequencies, and from local communications systems, to avoid interference with sensor response.

- The system should be light in weight and require low power so that it can be easily installed and carried on a small, economical airborne platform.

- Data reduction should be easy, relatively inexpensive and be accomplished in near real time.

These requirements are most nearly fulfilled by passive microwave radiometers and thermal infrared systems. Having identified the sensor types, further investigations using models and empirical data to determine the best system are warranted.

Microwave Applications Using Computer Models

The dielectric constant of soil is the single most important function in microwave sensing and should be understood when analyzing radiometric data. The general plan is to use soil dielectric properties to generate models by computer analysis, then combine the soil with water and oil using weighted averages and dielectric mixture theory for the included components. This leads to a realistic model which defines the expected response of microwave systems.

Emissivity, E, is a function of the complex dielectric constant, frequency and polarization. Since the frequency of any system used is set *a priori* only the complex dielectric constant and the effects of polarization need to be examined in detail.

Dry soils of different types have only slightly different complex dielectric constants at the same frequency. However, large changes in the dielectric constant of natural soils are observable by changing the interstitial fluids, such as increasing or decreasing the percentage of water saturation or changing the salinity of the fluids. This fact has been proven by many investigators and extensively studied by Lane, Saxton, von Hipple, and Kennedy. The models and data presented in this report are derived from, and based on measured dielectric properties of soil.

Computer Simulation of Effects of Oil and Water

The basic problem of detecting oil leaks in pipelines was approached using the obvious fact that oil would seep out of the pipeline and enter the surrounding soil and contaminate it to varying degrees. Interstitial water within the soil may be partially or totally replaced. This leads to an examination of the effects of adding various quantities of oil to dry soils and comparing these data with soils containing water. Then make a determination of the effects of oil/water mixtures on soils. Other variables are the frequency of operation, polarization effects and the angle of observation. In order to examine the effects of all these variables, families of curves were used along with the basic coordinate systems established for the presentation of radiometric temperature data. The system utilizes the radiometric brightness temperature as the ordinate and the observation angle as the abscissa for a given frequency. In this manner the behavior of different materials under the same conditions can readily be compared.

For example, Figure 1 shows the theoretical variation of microwave temperature obtained from a sandy soil as the interstitial water content is varied. An examination of these curves shows that two specific variations occur. As the water content increases, the microwave radiometric temperature decreases and the polarization contrast, ($\Delta T_P = T_V - T_H$), becomes larger. For instance the microwave temperatures at an observation angle of 45^o and 5% water have values of 278^oK for vertical polarization (T_V) and 221^oK for horizontal polarization (T_H). The differential, ($\Delta T = T_V - T_H$), is 57^oK. If the water content is increased to 10%, the vertical and horizontal temperatures decrease to 250^oK and 181^oK respectively, or a ΔT of 69^oK. Using both these phenomena, the moisture content of subsurface soils can be predicted with a high degree of accuracy(1).

Since the mechanisms of changing microwave temperatures with changes in moisture content are well known, what are the consequences if all or part of the interstitial water is replaced with oil?

Radiation in the microwave region is expressed as the radiometric brightness temperature, which is determined by:

$$(T_B)P = (1 - |R_P|^2)T_g \qquad (1)$$

---

(1) Microwave Radiometric Sensing of Soil Moisture Content; International Union of Geodesy and Geophysics, 14 General Assembly. International Association of Scientific Hydrology Division, Bern Switzerland September 1967.

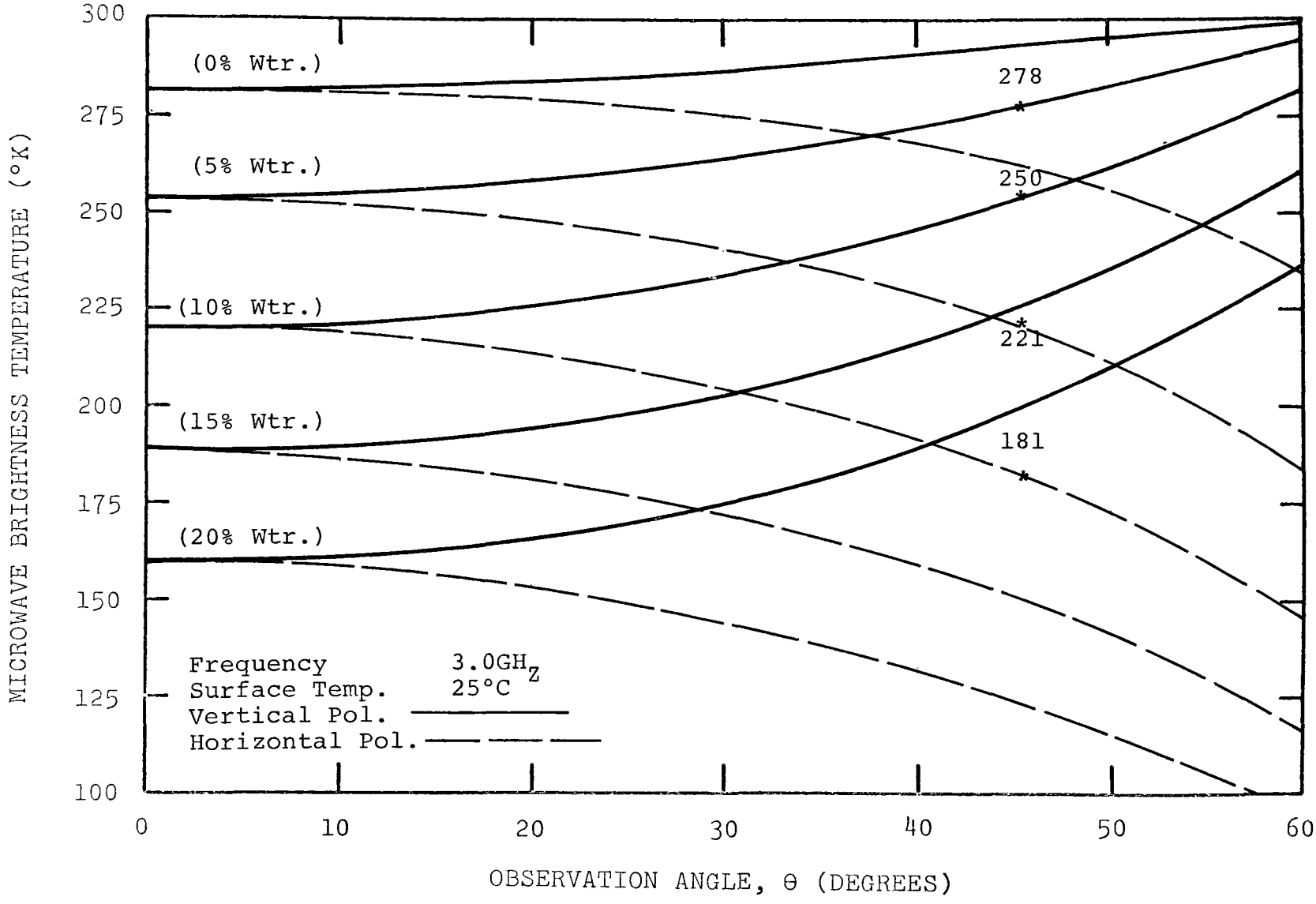

Figure 1 Microwave Temperature Variations as a Function of Changing Moisture Content.

where T_g is the ground thermometric temperature, subscript P stands for either the horizontal or vertical polarization and R_p is the complex Fresnel coefficient for horizontal or vertical polarization. The equations for the Fresnel reflection coefficients are:

$$R_H = \frac{\cos\theta - (\varepsilon - \sin^2\theta)^{1/2}}{\cos\theta + (\varepsilon - \sin^2\theta)^{1/2}}$$

and

$$R_V = \frac{\varepsilon\cos\theta - (\varepsilon - \sin^2\theta)^{1/2}}{\varepsilon\cos\theta + (\varepsilon - \sin^2\theta)^{1/2}} \qquad (2)$$

In (2), ε is the complex relative dielectric constant and θ is the nadir angle, i.e., the angle from the normal to the surface or the radiation observation angle.

The imaginary components of the complex dielectric constant, ε, for oils and other petroleum products is less by several orders of magnitudes than those for soil and water. A computer comparison in brightness temperatures, and polarization differentials between soil with oil and soil without oil, will suffice to show whether obvious local anomalies result from the presence of petroleum products.

For a sandy soil, at a representative ground temperature (25°C), at three selected microwave frequencies (0.3, 3, and 10 GHz), the horizontal and vertical brightness temperatures have been computed as a function of the viewing angle θ. This was performed for an array of combinations of soil, water and oil. Initial data for a representative oil selected from 17 petroleum oils is $\varepsilon' = 2.09$, and $\varepsilon'' = .0014$. ε' and ε'' are the real and imaginary components of the complex dielectric constant, with the convention that

$$\varepsilon = \varepsilon' - \varepsilon''\sqrt{-1}$$

Table 1 presents the measurements of soil and water as determined vy von Hipple (Reference (2)).

---

(2) Dielectric Materials and Applications, A. R. von Hipple The M.I.T. Press, Cambridge Massachusetts 1966 PP 314-315.

Dielectric Constants of Soil and Water

frequency (GHz) ⟶		.3	3	10
day sandy soil	ε'	2.55	2.55	2.53
	tan δ	.01	.0062	.0036
water	ε'	77.5	76.7	55.
	tan δ	.016	.157	.54
sandy soil 3.88% H_2O	ε'	4.50	4.40	3.60
	tan δ	.03	.046	.12
16.8% H_2O	ε'	20.	20.	13.
	tan δ	.03	.13	.29

TABLE 1

The "loss tangent", tan δ, is an alternative way of tabulating ε'':

$$\varepsilon'' = \varepsilon' \tan \delta$$

In order to employ equations (1) and (2) to evaluate brightness temperatures of sandy soil mixed with water and oil a weighted average based on oil/water content was used.

To establish the weighted averages, the horizontal and vertical microwave radiometric temperatures for soil with interstitial oil were computed as functions of frequency and observation angle. These data are shown in Figures 2 - 8 for 0.3 GHz, 3.0 GHz, and 10.0 GHz respectively. It is obvious that the horizontal and vertical microwave temperatures change drastically when interstitial water is replaced by oil in a soil. Another interesting point is that soil with oil maintains very nearly the same microwave temperatures, even though the frequency changes by an order of magnitude.

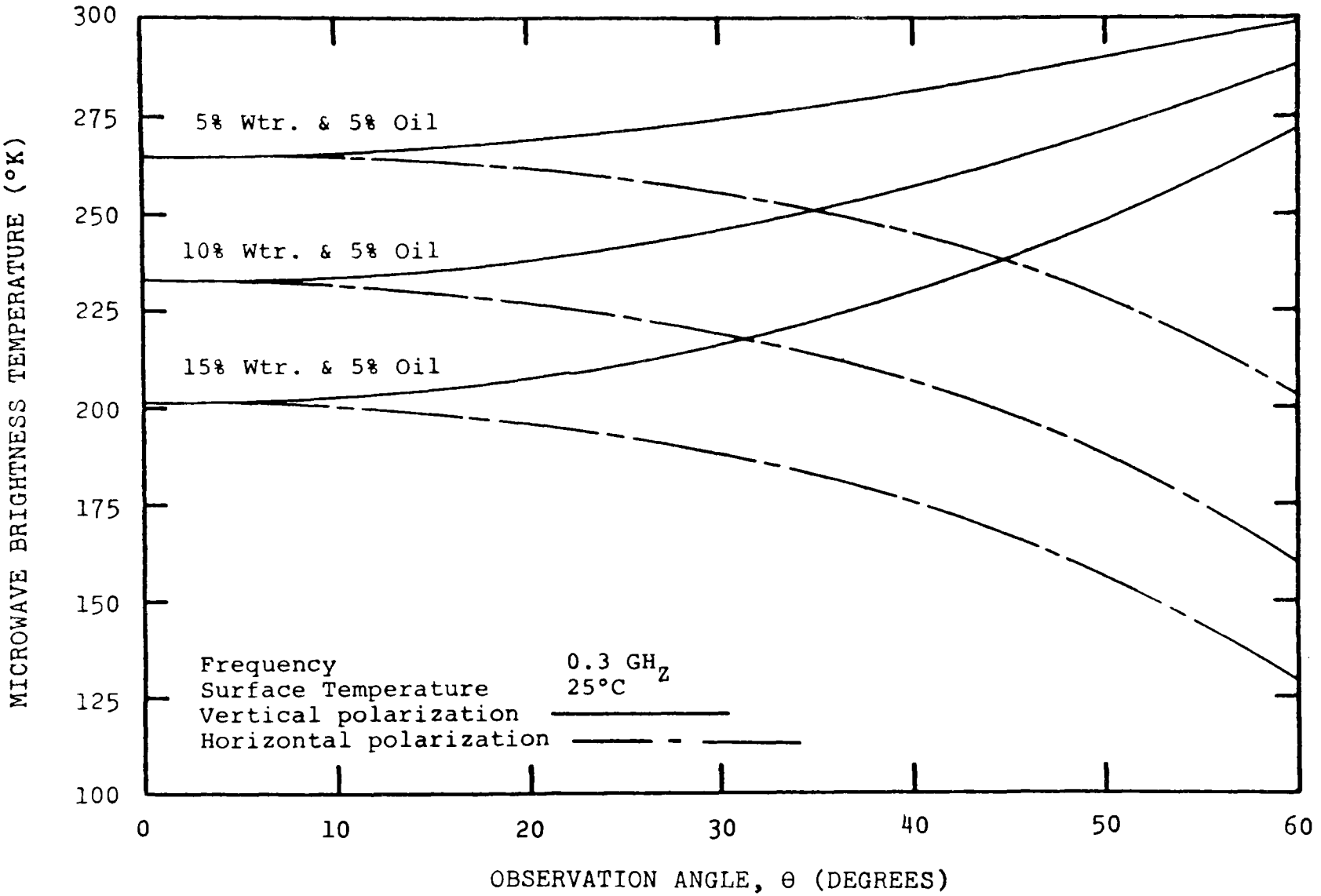

Figure 2 Microwave Temperature Variations as a Function of Changing Moisture and Oil Content

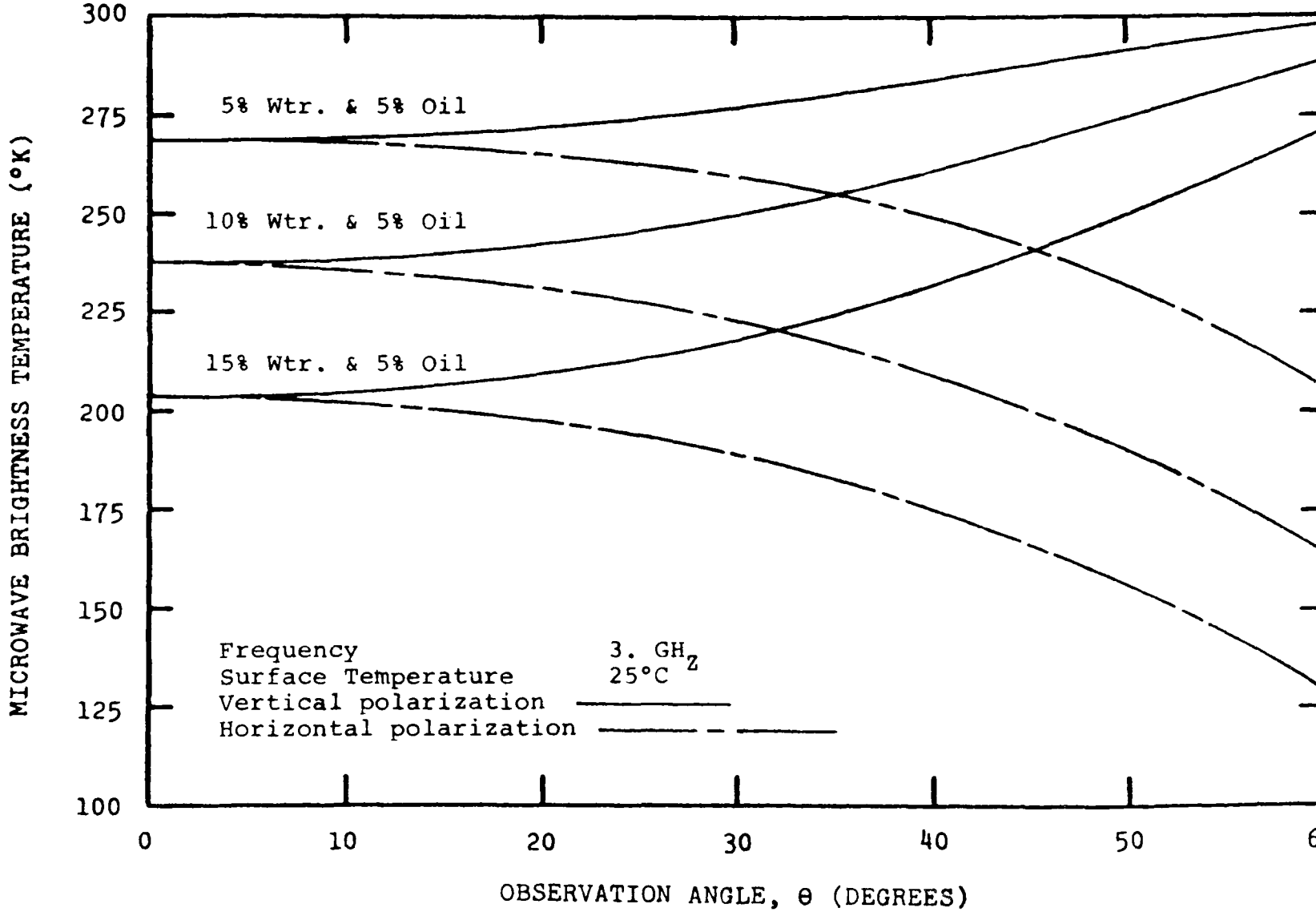

Figure 3 Microwave Temperature Variations as a Function of Changing Moisture and Oil Content

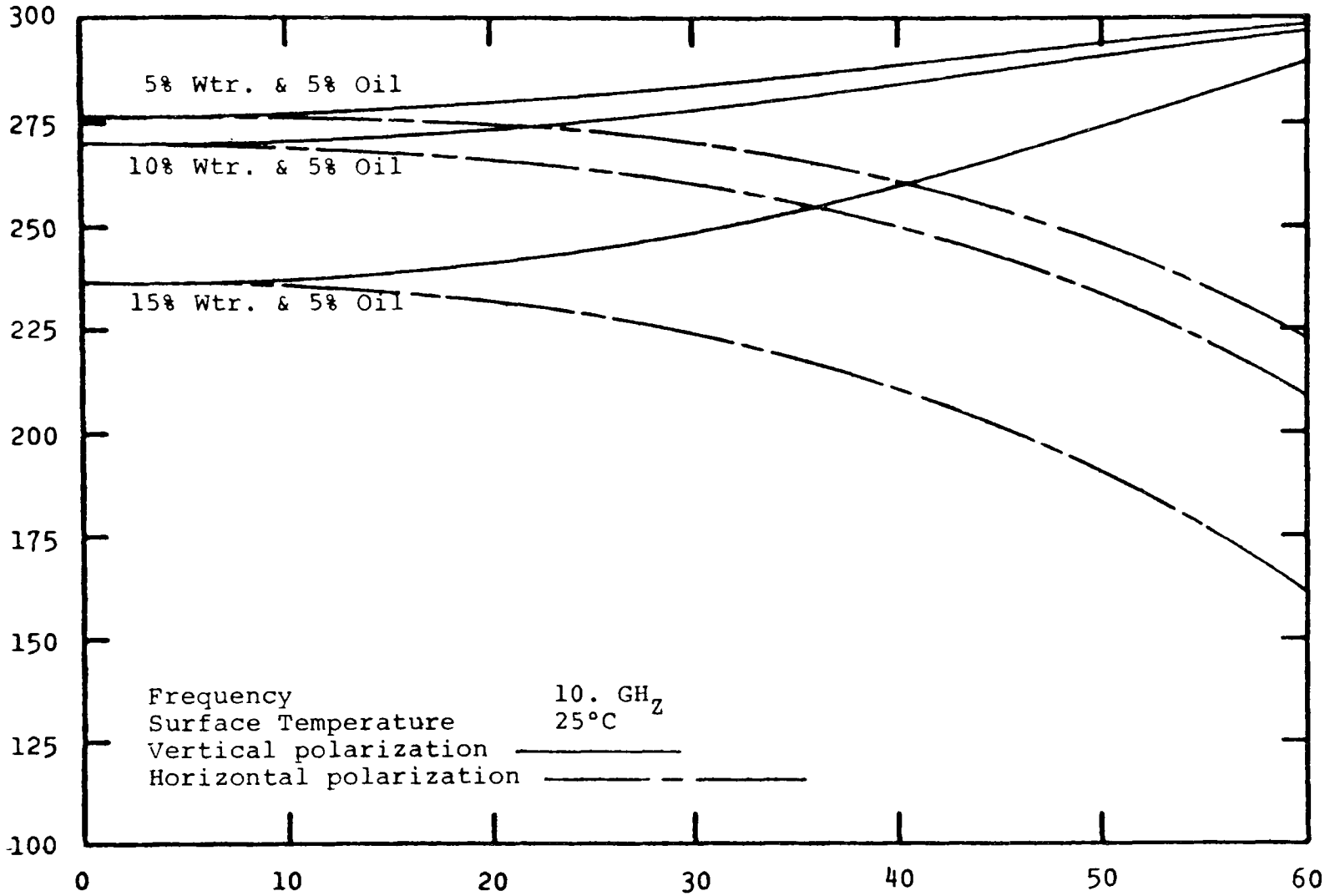

Figure 4 Microwave Temperature Variations as a Function of Changing Moisture and Oil Content

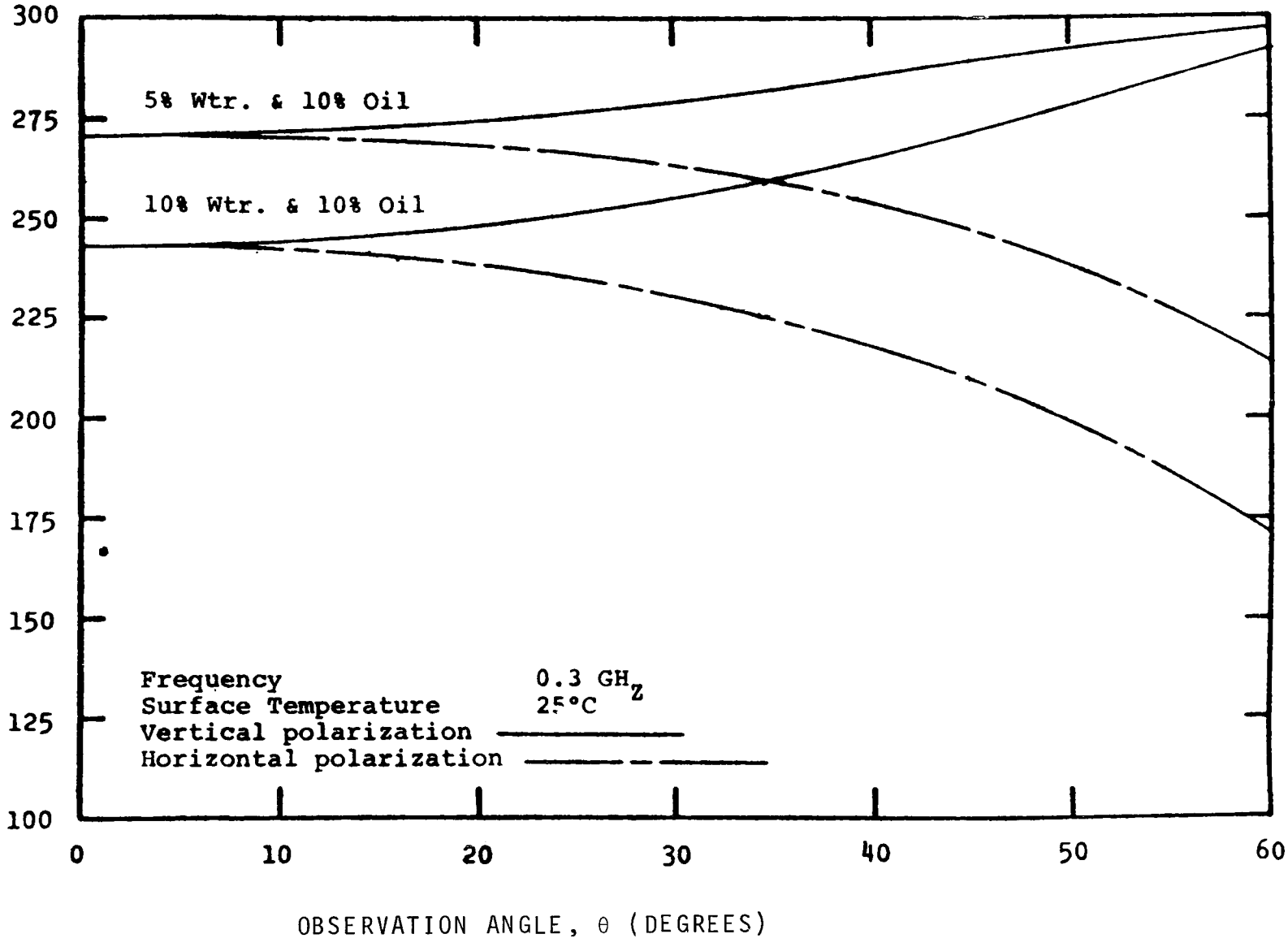

Figure 5 Microwave Temperature Variations as a Function of Changing Moisture and Oil Content

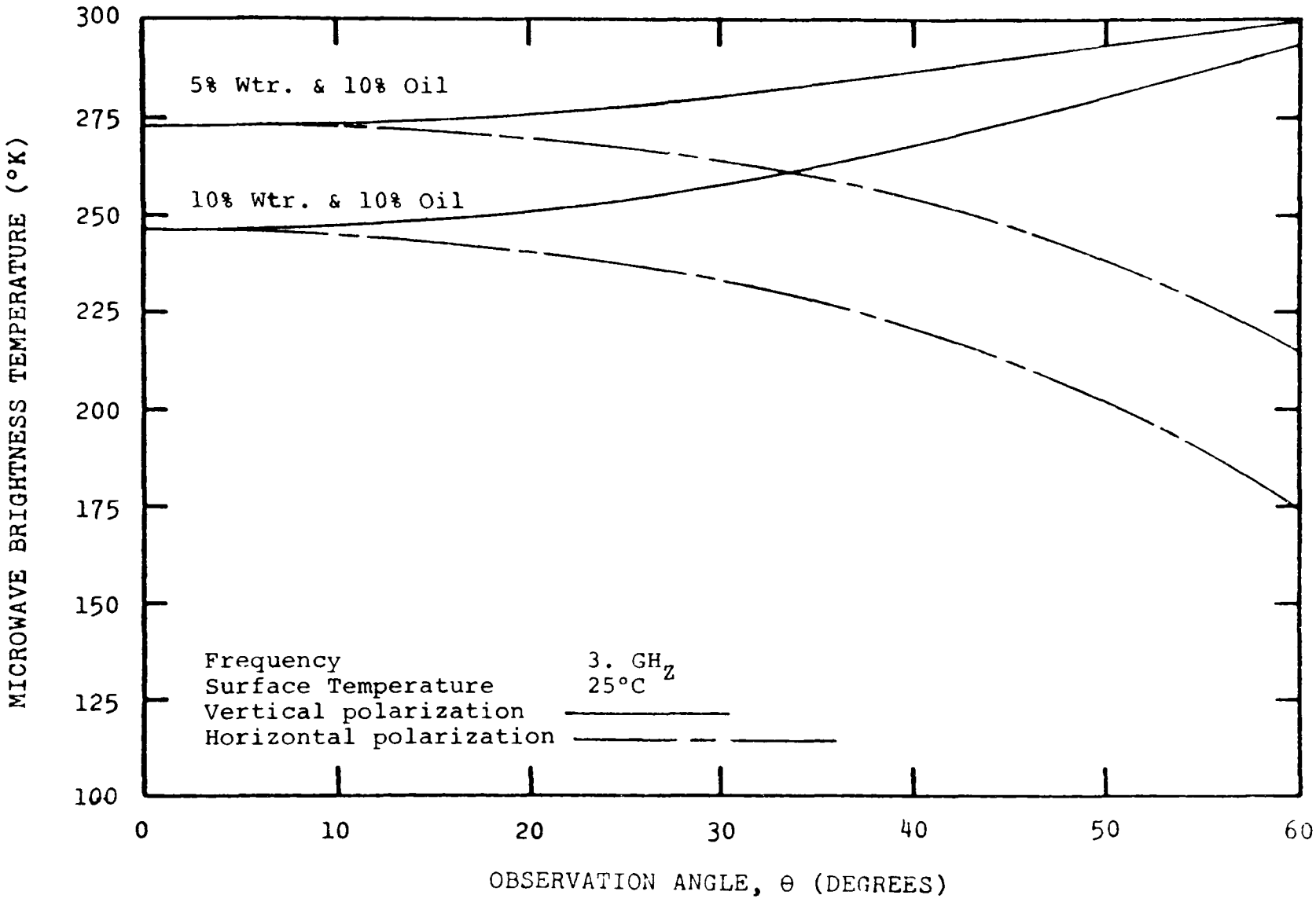

Figure 6 Microwave Temperature Variations as a Function of Changing Moisture and Oil Content

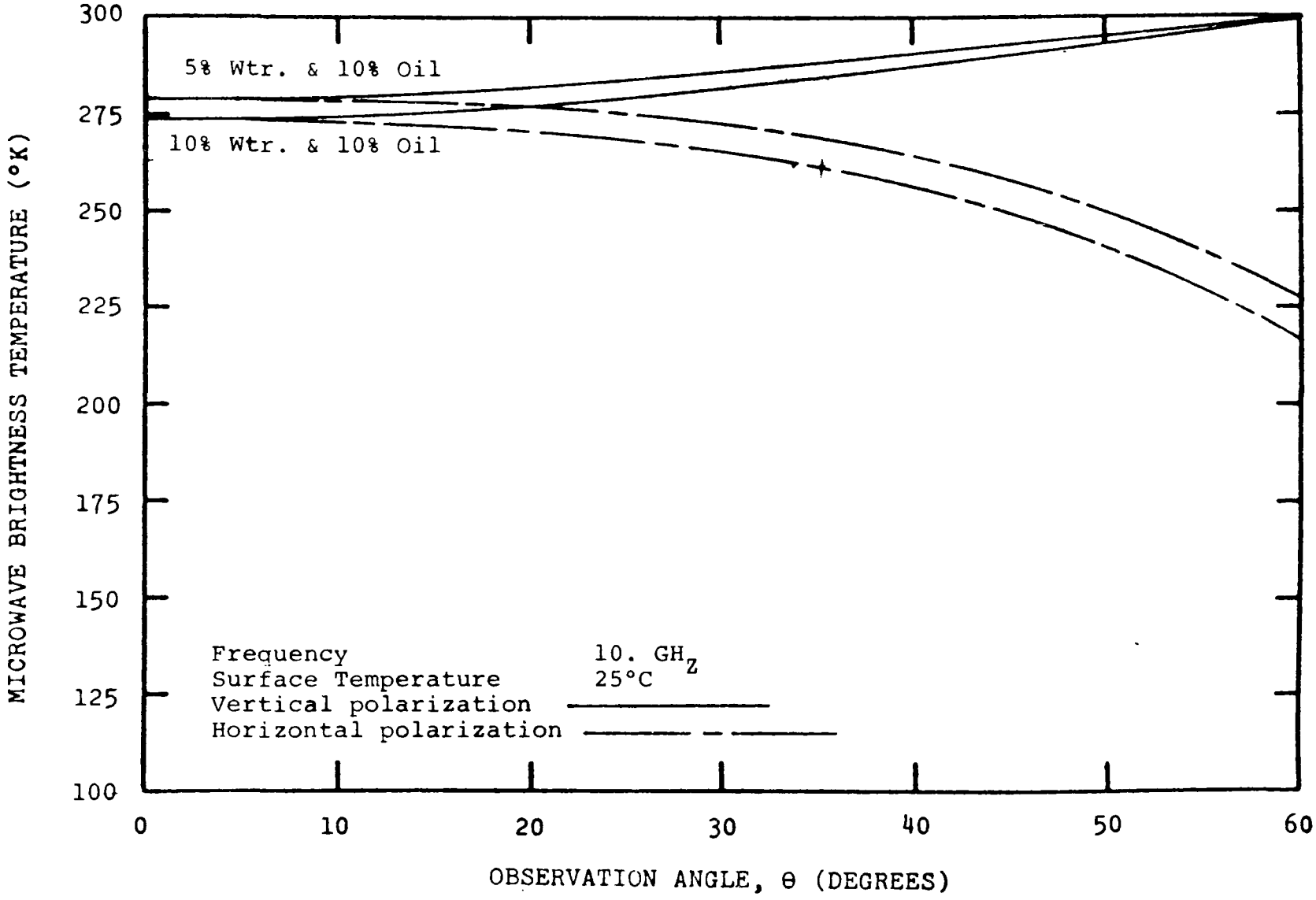

Figure 7 Microwave Temperature Variations as a Function of Changing Moisture and oil Content

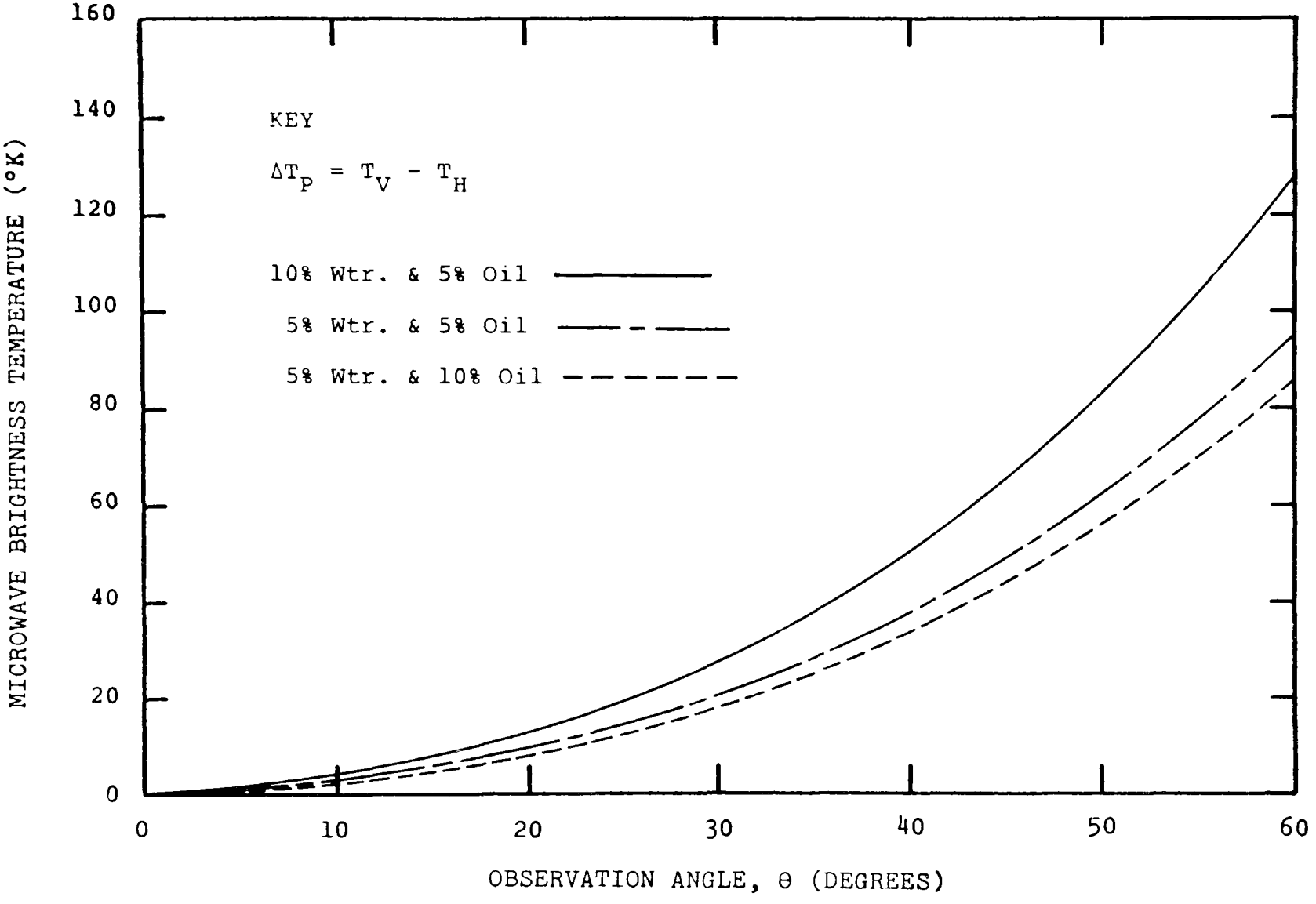

Figure 8 Polarization Contrast, ΔTp, for Soil Containing Oil and Moisture at 0.3 GH_z

Effects on Brightness Temperature and Polarization

Let us examine the effects of combining oil and water at 0.3 GHz (Figure 8). If we assume the sensor is pointed at 45° and the soil contains 5% oil and 5% water, the brightness temperature would be 286°K for the vertically polarized energy and 237°K for the horizontally polarized energy, or a ΔT_p of 74°K. These numbers are consistent with both theory and experiment and show there are actually two techniques of data analysis that can be used to define areas containing oil as an interstitial fluid. First, if oil is added to a soil, the microwave temperature increased sharply (in the above example from 254° to 286°K). Secondly, the polarization contrast is greatly reduced (in the above example from 74°K to 49°K).

Either one of the above functions may be used to detect oil leaks, but the possibilities of false alarms are greatly decreased if both functions are simultaneously observed. That is if a temperature increase is observed in conjunction with a decrease in polarization contrast, then it is almost certain that a dielectric with properties very similar to oil has been added to the soil..

Effects of Frequency

An examination of Figures 8, 9, and 10 show that microwave temperatures increase and polarization contrast decreases by the addition of oil are not restricted in frequency or by varying the oil/water content of the soil. In all cases the addition of oil caused an increase in microwave brightness temperature and a decrease in polarization contrast. It is interesting to note that as the specified frequency increases, the observed microwave temperatures become less variable and warmer. That is, the envelope of variability narrows even though the percentage of contained oil varies drastically. The same is true for polarization contrast. That is, the envelope of polarization contrast variability narrows considerably by increasing the (observation) frequency.

Signal and Resolution Considerations

The detectability of local warm spots will vary somewhat with the area or volume invaded by the oil. The invaded area must occupy enough of the radiometer beam ground intercept to register a significant change in radiometric temperature. For instance, if the invaded area is only one percent of the total area the radiometer receives radiation from, the anomaly will probably be hidden in fluctuations arising from natural heterogeneity.

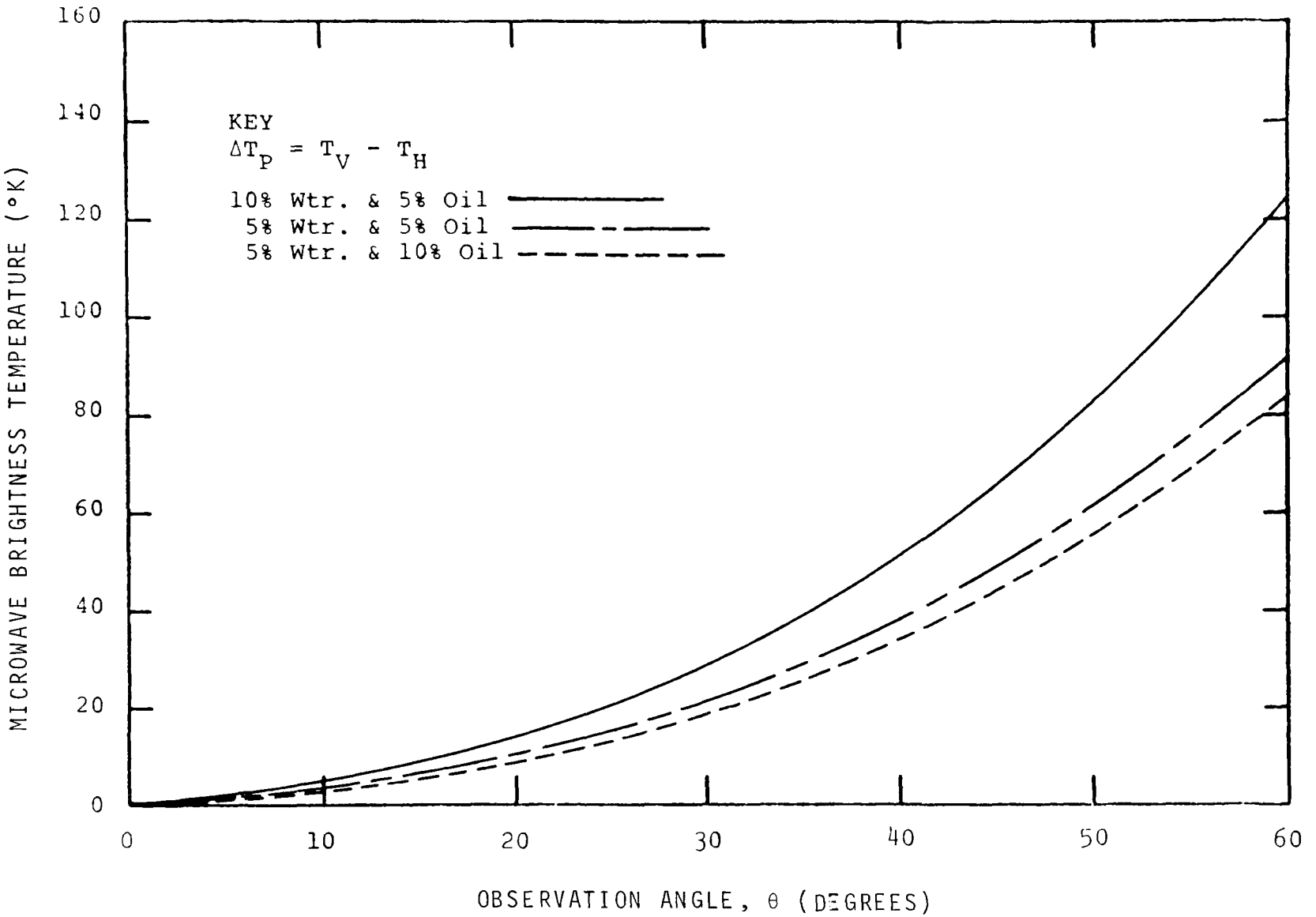

Figure 9 Polarization Contrast ΔT_P, for Soil Containing Oil and Moisture at 3.0 GH_Z

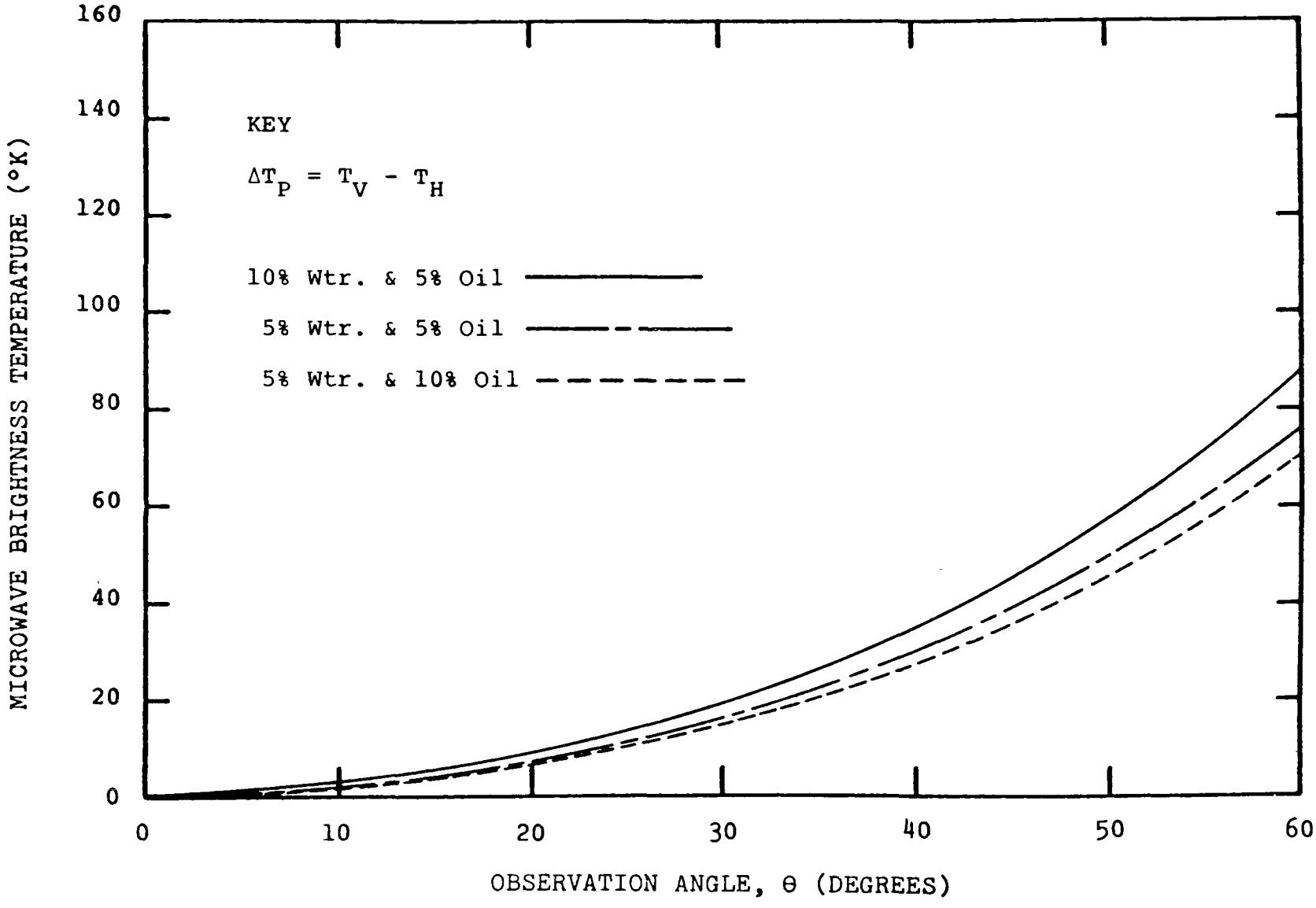

Figure 10 Polarization Contrast, ΔT_P, for Soil Containing Oil and Moisture at 10 GH_z

To estimate the size of warm areas required for a detectable anomaly, let the beam-filled area of a radiometer be denoted S, comprised of area A, with brightness temperature T_A, and area B, with brightness temperature T_B. Then the effective temperature combination the radiometer measures, T_S, is given by:

$$T_S = (A/S)\ T_A + (B/S)\ T_B$$

Table 2 presents some examples of microwave radiometric temperature predictions. In computing Table 2, an airborne system at 1000 feet altitude and having a 5^o beam width was assumed (a "worst case" condition).

d (feet)	Percent Oil			
	5%	10%	15%	20%
	Temperature Anomaly (^{o}K)			
20	.5	1.4	2.3	4.1
40	1.9	5.5	9.0	12.4
60	4.3	12.3	20.3	27.9
80	7.6	21.9	36.2	49.6

Computed Radiometric Temperature Differentials

Table 2

The magnitude of anomalies required to be distinguishable from background fluctuations is approximately 2^oK. However, this will vary with location and weather.

Effects of Varying Oil and Water Concentrations

Figure 11 is a generalized cross section of an oil leak in a pipeline, along with the microwave radiometric profile resulting from a survey. The following assumptions are made for modeling purposes:

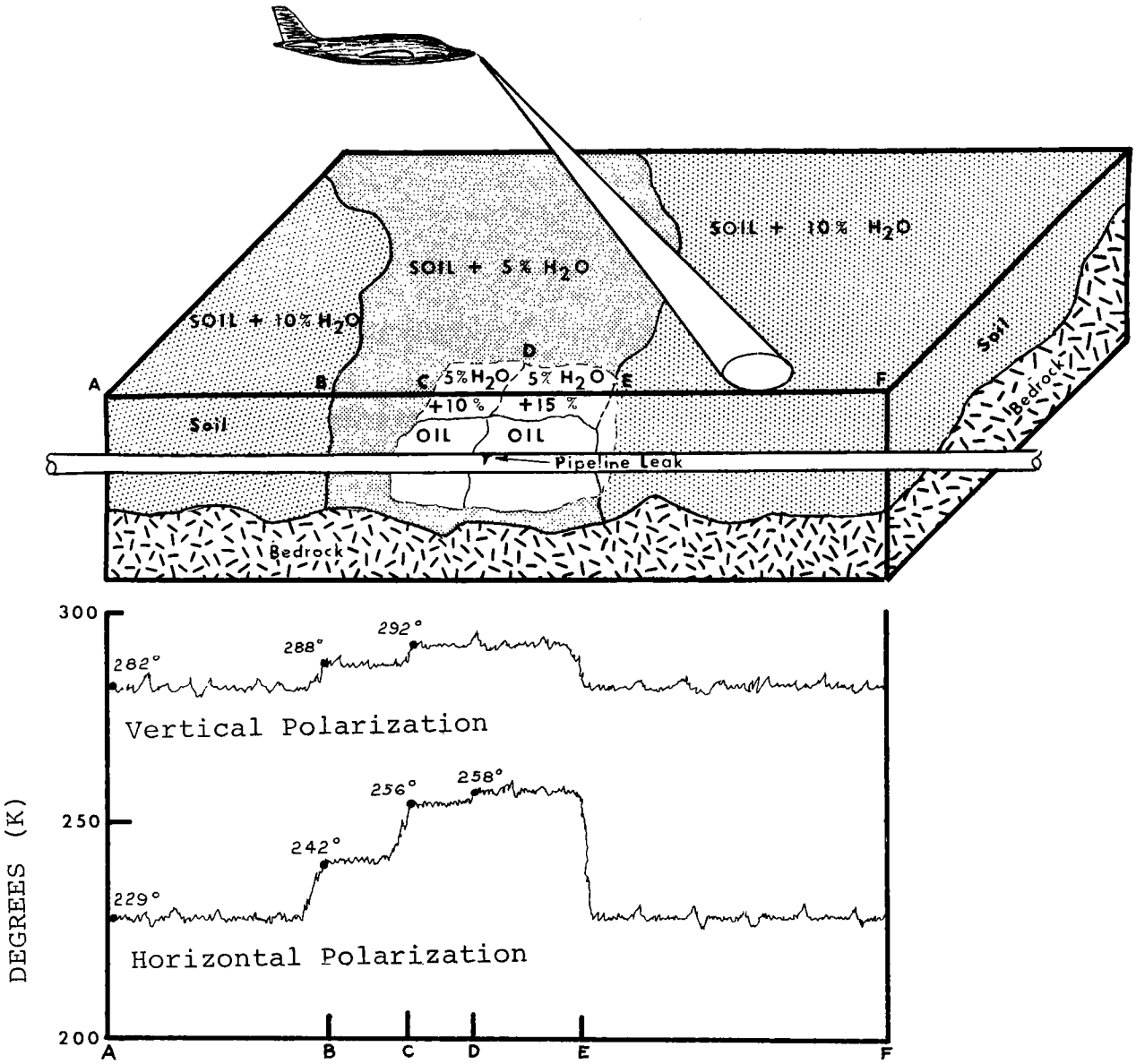

Figure 11 Computer Simulation of Pipeline Leak Detection

- The ground surface temperature is 25°C.
- The soil moisture is a variable 5 and 10 percent along the pipeline track.
- The subsurface dimensions of the oil intrusion fill the beam diameter of the microwave antenna.
- The operating frequency is 10 GHz.
- The observation angle is 45° (To obtain a polarization contrast $\Delta T = T_V - T_H$).
- The soil moisture and oil variability are (see figure):

  A to B - Soil with water only 10%

  B to C - Soil with water only 5%

  C to D - Soil with water 5%, oil 10%

  D to E - Soil with water 5%, oil 15%

  E to F - Soil with water 10%

This profile of horizontal and vertical microwave temperatures is a computer simulation of a flight along a pipeline and represents a model developed by using the developed data and theory.

The flight begins at point A and proceeds to point F with changes in water and water/oil content encountered along the flight path. Points B, C, D, and E represent the boundaries of these changes. The zone from A to B has a soil moisture content of 10% and is relatively cold both in the vertical and horizontal modes of operation. In the zone B to C, the soil moisture is decreased to 5% with the result that microwave temperatures increase both in the horizontal and vertical modes and a decrease in polarization contrast is observed. From C to D the total fluid content is 15% (5% water and 10% oil). If this were all water, cold microwave temperatures would be registered along with a large increase in polarization contrast. However, the addition of oil has the effect of increasing both the horizontal and vertical temperatutes, with the horizontal component increasing much more than the vertical. Therefore, a large decrease in polarization contrast is realized. From D to E, the fluid content is again increased by additional oil. While the vertical temperature is increased very little, the horizontal temperature increases a significant amount, resulting in a further decrease in polarization contrast. From E to F the soil contains only water (10% and the same microwave characteristics are

observed as from A to B, which also contains 10% moisture.

Infrared Measurements

Other than photography, probably the most advanced imaging systems, in a hardware sense, are thermal IR imaging systems. However, these systems lack some desirable features for petroleum product leak detection. First thermal IR does not penetrate to significant depths and must depend on secondary thermal effects that migrate to the surface for detectability. Secondly, IR is not all weather, rain, fog, snow and haze affects the data. Thirdly, the ability to detect any phenomena by IR is time dependent. That is, most successful IR data is obtained at night or in the early morning hours when solar reflections are absent.

The value of IR imaging in conjunction with microwave surveying for leaks comes from its ability to detect the secondary thermal effects of a buried pipeline with almost photographic resolution. This fact is firmly established and is very apparent from the obtained field data.

SECTION IV

FIELD MEASUREMENTS PROGRAM

The field measurements program was divided into three primary phases:

- Area reconnaissance and site selection.
- Experiment design.
- Airborne and ground measurements.

Each of these major phases are sub-divided into subject groups for discussion purposes.

Area Reconnaissance and Site Selection

A number of major pipeline companies were contacted in an effort to determine areas that could be used as test sites. Two major pipeline companies were very cooperative and not only furnished detailed records of petroleum leaks but also directed a number of field engineers to support the study. Six areas were examined as potential test areas. Two were in Brazos and Robertson Counties about one hundred miles northwest of Houston, Texas. These areas were very densely vegetated with both trees and underbrush. Since a multiple canopy exists, this probably would represent a "worst case" situation for demonstration purposes. The areas were not rejected, but set aside for test flights at a later date.

The other four areas examined were in west Texas about forty miles west of Odessa, Texas. Two were in Crane County and two in Winkler County. From these, two sections of pipeline, each approximately two miles in length, were selected in Winkler County and one, approximately one and one-half miles in length, in Crane County. These areas were selected for several reasons, but primarily because:

- A variety of leaks, old and new, were present and well documented.
- The leak areas and pipeline sections had not been disturbed to any great extent.
- Some leaks are readily visible while others are hard to detect visually.

- Both compact and low density soils are represented.
- Accessibility was relatively easy.
- The flat terrain allowed easy location of the sites from the air, especially at night.
- The selected pipeline sections were relatively straight trunk lines.
- Both small and large diameter pipelines were represented.
- Population density is very low (open range land).
- Nearby airfield facilities are present.
- Land owner permission to enter is easily obtained.

Terrain, Geology (surface) and Geography

Six individual leaks were identified along a one and one-half mile section of pipeline right-of-way in Crane County. Actually there are two parallel eight inch trunk lines used primarily to transport crude oil. The leaks occurred at various times between November 1968 and March 1970.

The terrain is gently rolling sand hills with occasional intermittent stream cuts. The sand dunes are recent, underlain by quaternary alluvium which rests, unconformably, on Triassic red beds. Together the dunes and quaternary alluvium are 30 to 100 feet thick. In general the regional soil maps indicate simply "sand dunes" for the area. The dunes are very immature and readily move in the direction of prevailing winds. They are highly permeable and move on caliche beds five to thirty feet below the surface. The thickness of soil covering the caliche is highly dependent on dune development. The caliche is generally flat and horizontally planar. In many places the pipeline, which was originally buried, is now exposed due to dune movement.

The base elevation for the region is about 2600 feet, with variations due to sand dunes, rolling hills and intermittent streams. The climate is semiarid with about fourteen inches of annual precipitation, concentrated in late summer. In June, when the survey was conducted, the average rainfall is less than two inches. Low rainfall and high permeability were excellent for testing the sensors under dry, low soil moisture conditions.

The population density is very low. Land use is confined to open range cattle grazing (ranching) and oil production. No farming occurs anywhere in the general area.

The other two pipelines selected are in Winkler County near the town of Kemit. There are about fifteen identified petroleum leaks with these two test sites. These occurred over a period of time from November 1968 to April 1970.

The terrain is very flat with some gently rolling hills. The surface soil is a fine loamy sand known as the Springer unit. This soil packs well and in general is relatively firm. However, when the surface crust is broken it becomes soft and dusty. Sand dunes of the type encountered in Crane County are rare. The Springer soil unit is a residual of Quaternary alluvium which is 80 to 200 feet thick and rests unconformably on triassic red beds. Fifteen feet below the surface there is a caliche horizon that is 10 to 20 feet thick. Soil maps of the area are in conflict, some maps showing sand dunes, some barren of sand dunes. Area reconnaissance did not locate any dune sand areas. Groundwater occurs unconfined in the Quaternary alluvium at 70 to 100 feet.

Other parameters such as rainfall, vegetation, land use and general geography are the same as that found in Crane County.

Vegetation and Water

Vegetation is sparse and widely scattered as in most semiarid areas. There are no trees of any kind in the area. Plants, where present, are mostly sage brush, mesquite, shinoak, and clumps of long bladed grass.

Water is sparse, highly mineralized, and derived mainly from deep-water wells. Although the water table is only 60 feet at the test sites, it occurs unconfined in Quaternary alluvium, and is not potable because of mineralization.

Airport Facilities

Two airfields of significant size are located in the general area, one at Monahans and Midland International Airport. For the instrumented aircraft used on this survey it was highly desirable to use the complete facilities at Midland International.

Aircraft and Instrumentation Selection

Five requests for bids were sent out to various companies known to have airborne remote sensor systems of the types desired. Based on abilities to meet instrument and flight specifications two (2) contractors were accepted, North American-Rockwell, Downey, California and Remote Sensing Inc., of Houston, Texas.

The North American-Rockwell aircraft was to fly low altitude missions at the same time RSI was flying higher altitude missions. During the first pre-mission instrument checks the North American-Rockwell instrumentation was found to be inoperative and repairs could not be instigated in time to obtain simultaneous airborne and ground data. Since the three (3) ground crews and site markings were already in place it was decided to use only the RSI instrumented aircraft at an intermediate altitude, about 1000 feet.

The RSI aircraft and instrumentation specifications are as follows:

1. Aircraft:

   Fan Jet Falcon

   Wing Span - 53.3 feet

   Length - 56.25 feet

   Height - 17.75 feet

   Landing Weight - 26,956 lbs.

   Maximum Gross Weight - 27,300 lbs.

   Engine (2) thrust - 4,250 lbs. each

   Landing Speed - 125 mph

   Cruise Speed - Mach .76

2. Instrumentation:

   a. Ryan Model 703, 13.7 GHz Radiometer

      Antenna Gain - 31 db

      Beamwidth (3 db) - 5 degrees

Polarization - Horizontal or Vertical (selected)

Viewing Angle - 45^{o} aft (relative to horizontal aircraft axis)

Overall Linearity - 0.1% max.

Operational Temperature - (-) 50 degrees C to (+) 50 degrees C

Sensitivity- 0.3^{o}K (one second integration time)

Absolute Accuracy - 2 degrees K (nominal)

Baseline Stability - 2 degrees K/hr (max)

Temperature Measurement Range - 190 degrees K to 450 degrees K

b. Texas Instruments RS-14 Infrared Scanner

Operational Temperature - (-) 40 degrees C to (+) 50 degrees C

View Coverage - (±) 40 degrees lateral

Noise Equivalent Temperature - 0.3 degrees C

Scan Rate - 200 Scans/second

Velocity to Height Ratio - 0.02 to 0.2 Radians/Second

Stabilization - Roll ± 8 degrees

Detector Cooling - Closed cycle, 26 degrees K

Calibration - Continuous (black body)

c. Camera System - Four 500 EL Hasselblad

70mm cluster

Film Format - 70mm

Field of View - 52 degrees

Lens - Zeiss Planar

Aperature - f/2.8

Focal Length - 80mm

Shutter Speed - to 1/500 sec.

Magazine Capacity - 100 ft. (each camera)

Exposure - Four cameras simultaneously

Film types - Kodak 2402, 2424, 2448 and 8443

d. Recording System

The recording system is an individual unit specially constructed to meet the demands of all remote sensor systems on the aircraft. All available instrumentation was not utilized on this experiment. Basically, the recording system is built around a Precision Instrument fourteen-channel tape recorder. All necessary timing and ancillary information is recorded simultaneously with the data gathering function. This insures that all data can be properly oriented in time and space and data offsets are avoided during the reduction operation.

Ground Correlation Instruments

Prior to performing the survey it was determined that the only ground parameters that may be necessary to correct or verify the airborne data was ground temperature, soil moisture content and soil hydrocarbon content.

Ground temperature was obtained at the surface and ten (10) inches below the surface using special steel shaft soil thermometers. The surface temperature was obtained by horizontally inserting the sensor tip a fraction of an inch below the soil surface so that it would not be perturbed by direct sunshine impinging on the detector element. Three full minutes were allowed to insure an equilibrium measurement. Adjacent to each surface measurement a four inch hole was dug out and the six inch shaft forced into the soil to obtain the temperature at ten (10) inches below the surface.

Soil moisture was obtained at the surface and at a depth of ten (10) inches by collecting a quantity of surface soil and placing it in a sealed aluminum container. The ten inch grab samples were obtained by digging a hole and taking soil samples from the sides of the hole. These samples were then placed in individual aluminum sample containers and labeled accordingly. Water content was determined by using well known heating and weighing

techniques. All water content measurements are in percentage by weight.

Hydrocarbon content was measured at several leak sites for each of the three sections of pipeline overflown. The samples were obtained in the same manner as the soil moisture samples. However, the hydrocarbon content was determined by Core Laboratory Co., in Houston. The method used was standard combustion techniques used by the oil industry, also in percentage by weight.

The obtained data are reported in Section VI, Data Analysis and Interpretation.

Site Markings

The test sites were marked with a variety of materials to aid both flight crews in identifying the test locations from the air and to aid in the interpretation of data.

The three test sites were marked basically in the same manner. "T" markers were used at the beginning and end of each test site for flight crew orientation. The "T" markers were 80' x 50' white paper towels that pointed towards the leak areas (Figure 12).

The next marker used was 2800 square feet of aluminum foil. The aluminum foil was used to provide additional flight crew guidance and as a distinctive marker for the microwave radiometer and thermal IR imagery. The aluminum foil was laid out perpendicular to the pipeline in 18 inch wide strips 25 feet long and 18 inches apart (Figure 13).

Each leak was marked by four 30 foot strips of white paper towels at angles to the pipeline to form a tie mark for additional flight crew orientation (Figure 14). Strips of white paper towels were laid out along the pipeline for flight crew guidance. A schematic of the marking system is shown in Figure 15.

At night the right-of-way was marked by a series of lights. The beginning of each line was marked by a flashing red strobe light with white flashing strobe lights placed at regular intervals along the pipeline. The end of the site was marked with three highway flares placed in a triangle. All of the night markings were for flight crew guidance with the exception of the aluminum foil, which was used as a correlation point.

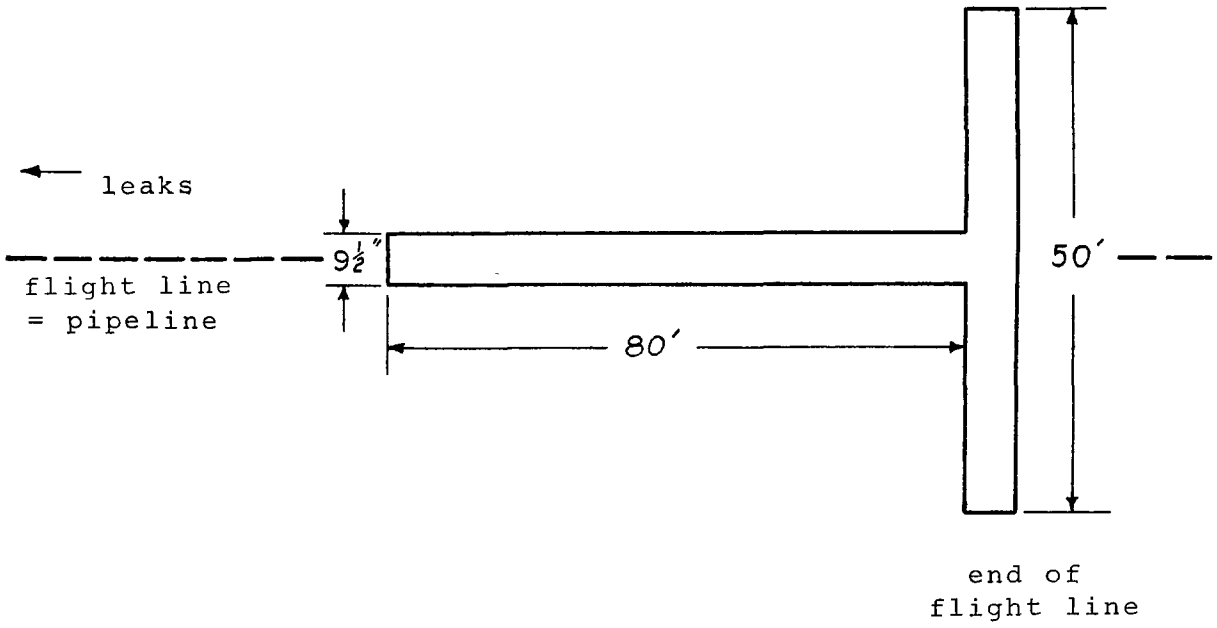

Figure 12 End of Flight Line Markers

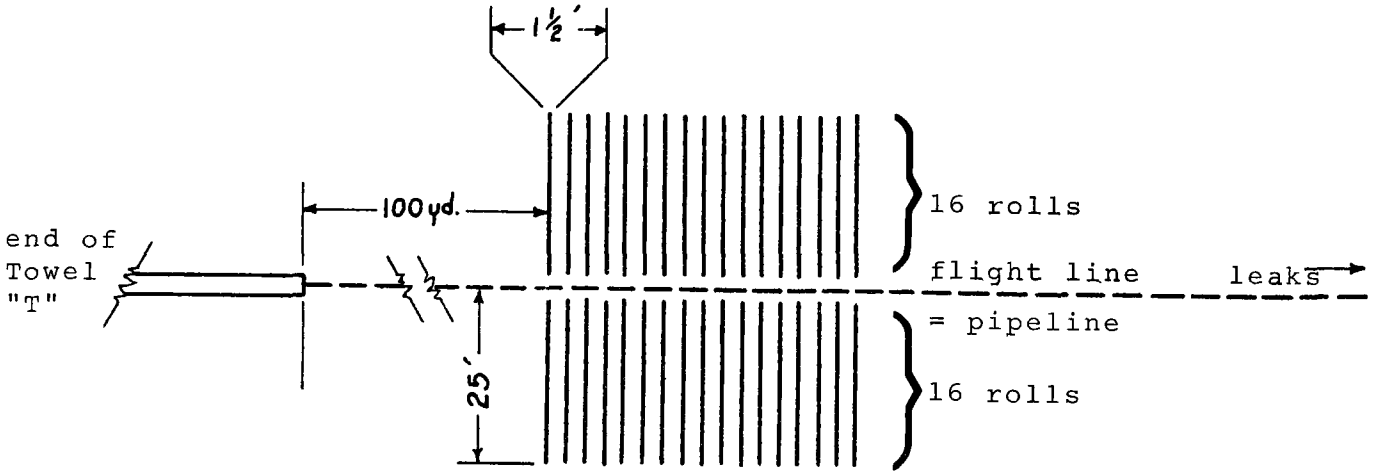

Figure 13 Aluminum Panel Electromagnetic Markers

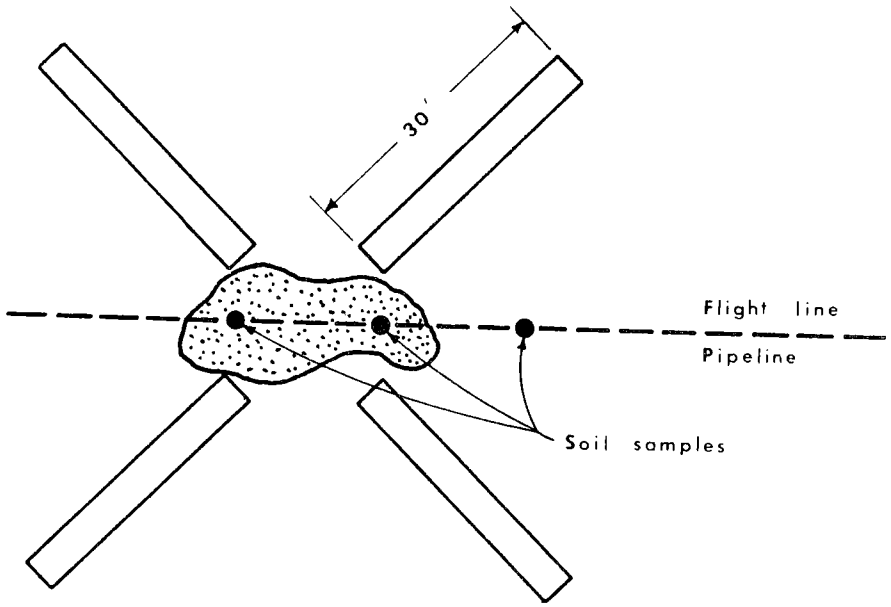

Figure 14 Leak Site Identification Markers

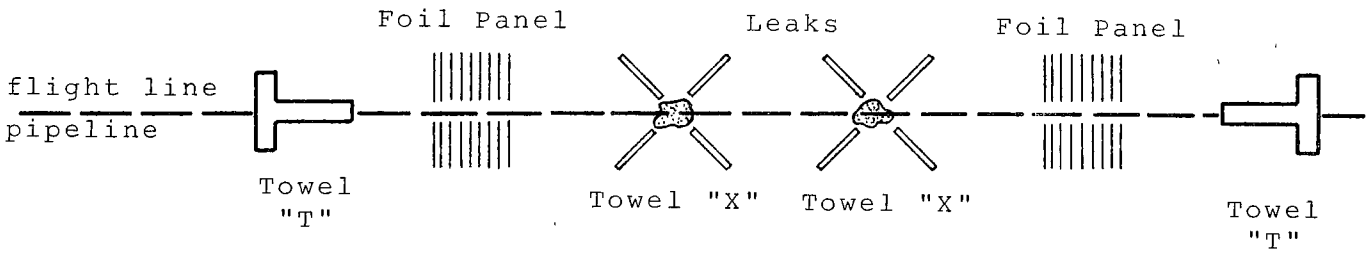

Figure 15 Schematic Diagram of a Test Site

J-0014 SCHEDULE

Tuesday, June 9, 1970

Leave Nassau Bay, 4:00 P.M.
Drive to Midland, Texas
Arrive approximately 11:30 P.M. - 12:30 A.M.
Stay at Holiday Inn Motel in Midland

Wednesday, June 10, 1970

Breakfast 6:00 A.M.
Proceed to test sites, mark route, take soil samples.

Party No. 1 - Crane Test Site
Site 1: 3-mile stretch of 8-inch and 10-inch pipeline in northwest Crane County. southeast of county road 1223, halfway between Crane and Monahans (see map). Place "T's" and foil panels at each end of line, mark and sample six leaks.

Party No. 2 - Site Southeast of Wink
Site 2: 3-mile stretch of 6-inch pipeline 2-3 miles southeast of Wink, between pipeline patrol stations S9 and S15. Place "T's" and foil panels at each end of line, mark and sample five leaks (see map).

Party No. 3 - Site East of Wink
Site 3: 2-mile stretch of 8-inch pipeline northeast of Wink, between railroad and black top road (see map). Place "T's" and foil panels at each end of line, mark and sample large leak area.

Thursday, June 11, 1970

8:00 A.M. - Brief airplane crews at airport on test site locations, flight line markings, daylight flight procedures.

10:00 A.M. - Noon - ground parties proceed to test sites, take surficial and deep soil temperatures, record in field books.

Noon - 1:00 P.M. - Daytime overflight. Afterwards, take soil temperatures again, and record.

7:00 P.M. - Brief airplane crews at airport on night overflight.

10:00 P.M. - 12:00 Midnight - Set up strobe lights at ends and in middle of flight lines (3 per line).

12:00 Midnight - 1:00 A.M. Take and record soil temperatures.

Friday, June 12, 1970

1:00 - 2:00 A.M. - Night overflights

2:00 A.M. - 4:00 A.M. - Take and record soil temperatures, pick up route markers, leak markers, strobe lights, etc.

12:00 Noon - 5:00 P.M. - Return to test sites and clean up foil, paper and other trash. Also remove survey markers.

Friday evening or Saturday - Return to Houston

J-0014 PILOT ORIENTATION

The mission is to overfly three sites in Crane and Winkler Counties, Texas, about twenty-five to fifty miles south and west of Odessa. Directions, distances, and orientation features are as follows.

Daytime Flights

Site 1 is in northern Crane County, about fifteen miles northwest of the town of Crane. It is in the eastern edge of a sand dune area. Flying along a bearing of 290°, the pilot will see a green smoke bomb marking the start of the line. Next will be a "T" made of white paper towels, with the stem of the "T" pointing northwest. One hundred yards further will be a 50' x 50' aluminum foil marker. He will see a number of white towel "X'x", marking the flight line. Next will be another aluminum foil marker panel, a towel "T", and a red smoke bomb to mark the end of the line.

Proceeding thirty miles west and north, passing over the town of Monahans, he will come to Site 2. Flying on a bearing of 320°, he will see another green smoke bomb followed by a towel "T", next a 50' x 50' aluminum foil panel. Again, a number of white "X's" will further delineate the flight line. Coming to the end of the line, he will see another aluminum foil panel, a white towel "T", and a red smoke bomb which marks the end of the line.

Site 3 extends along a bearing of 49°, and is about five miles northeast of the end of Site 2. The pilot will see a green smoke bomb just east of a railroad, marking the start of the line. Next will be a towel "T", then an aluminum foil panel, then one

large white "X". Approaching the end of the line, he will see an aluminum foil panel, a white towel "T", and finally a red smoke bomb. Figures 16, 17 and 18 are detailed lay-outs of each site to be surveyed.

Nighttime Flights

Approaching Site 1 from Crane along a bearing of 290°, the pilot will see a flashing red strobe light, which marks the start of the line. Further along the line he will see three blinking white lights. Red flares mark the end of the line.

Flying north and west over Monahans as during the day, the pilot will see a flashing red strobe light marking the start of Site 2. A line of three blinking white lights will extend along a bearing of 320°. Red flares will mark the end of Site 3.

Turning northeast and flying along a bearing of 49°, the pilot will see a flashing red strobe light, marking the start of Site 3. Three blinking white lights will further mark the site. Red flares will mark the end of Site 3.

Flight Tests and Ground Data

The flight schedules and ground data gathering proceeded as scheduled with no problems or significant errors. The desired results were completely realized with exception of site #3, where night ground data were not obtained because of vehicle difficulties.

The outcome of the flights and comparisons with ground data are contained in Section VI, Data Analysis and Interpretation.

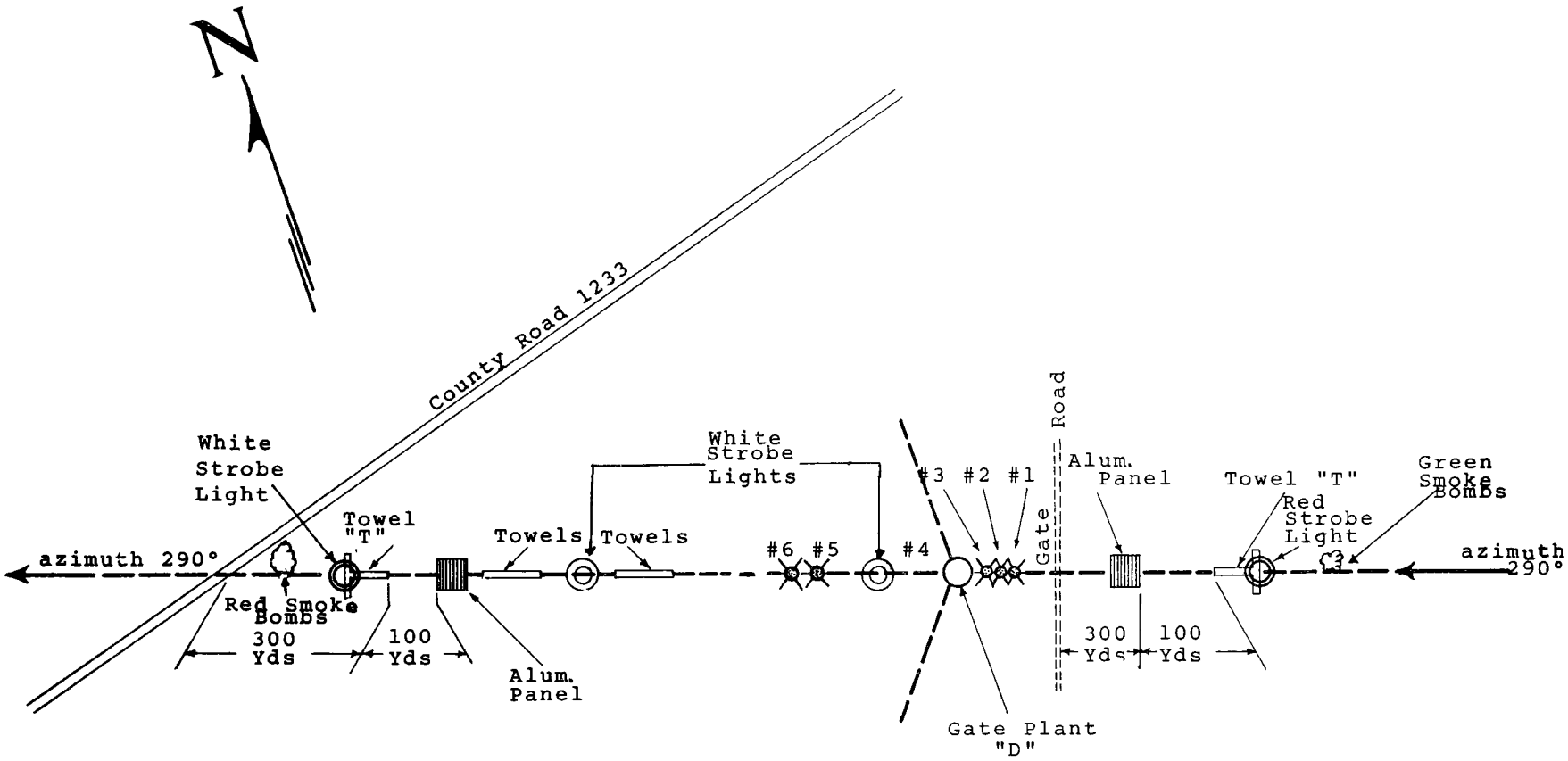

Figure 16 SITE 1 West of Crane, Crane County, Texas

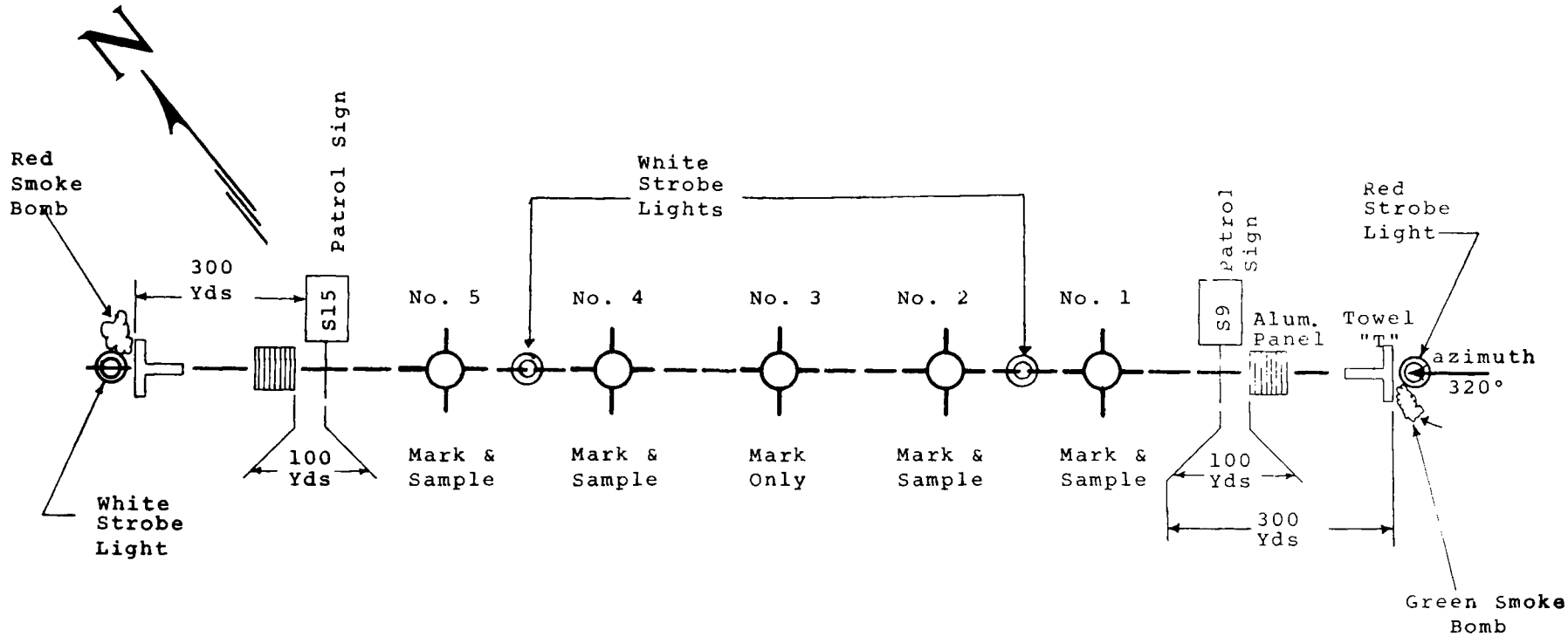

Figure 17 SITE 2 Southeast of Wink, Winkler County, Texas

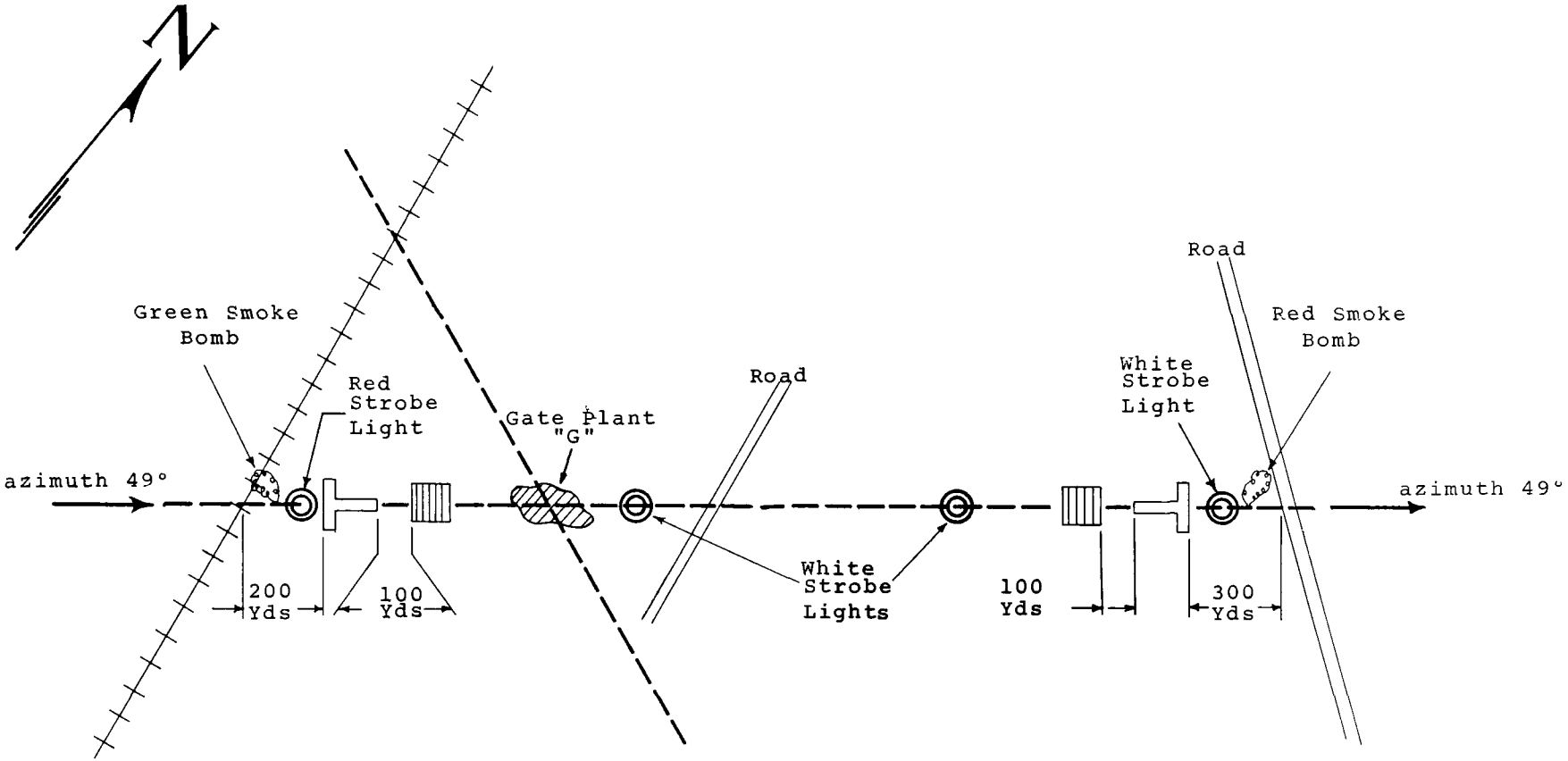

Figure 18 SITE 3 East of Wink, Winkler County, Texas

SECTION V

DATA CORRELATION AND REDUCTION

The correlation of the data from the six sensors is accomplished using both photogrammetrics and elapsed time. The black and white photography, the black and white photographic IR, the color photography and the photographic color IR are individually mosaiced into uncontrolled strips. The four strip mosaics are then photogrammetrically tied together using numerous checkpoints to assure accurate alignment. The correlation of the thermal infrared with the photographic sensors is accomplished by dividing the former into high interest sections, such as a leak area, and then matching the sections to the corresponding areas on the photograph.

The correlation of microwave profiles with thermal infrared and photographic images was attained by a 400 Hz signal generator which drives a light source internal to the infrared system and simultaneously puts a 400 Hz signal across all 14 tracks of the recorder system. Two of these timing dots occur at the beginning of each data run and three at the end. This permits an exact correlation between a particular infrared scan line and a particular microwave radiometric temperature value. Also, each data strip of thermal infrared imagery is coded by a margin light source. This coding identifies mission, time and flight number. The infrared and photographic images are visually aligned so that all required data is correlated. In order to doubly insure proper correlation between all systems, large aluminum panels were placed on the ground. These panels, at the beginning and end of each section of pipeline surveyed, caused large cold anomalies to occur in both the infrared and microwave radiometric night data and readily observed in daytime photography. Although the aluminum panel system works well for both day and night operations, it was designed primarily to ensure both data correlation and target acquisition during the night missions. Also, the measured distances between markers and the size of the markers were used to establish accurate scale factors.

The entire system worked very well with the exception that the aluminum panels were not, in all cases, intercepted by the microwave radiometer beam pattern.

Calculation of Scale

An important factor in photographic interpretation is accurate determination of scale. Scale is the relationship between distances on maps, graphs or photographs and the actual ground

distance. It is normally expressed in one of three ways; either as a representative fraction in which the numerator is unity, such as 1/10,000, or as a ratio 1:10,000 or in dissimilar units 1 inch equals 1 mile. The representative fraction and the ratio one unit on the map or photo equals 10,000 units on the ground.

The scale of the photography was determined by ratioing known distances on the ground to the distance on the photograph. The primary instruments used to calculate scale factors for each flight line was the measured distances between ground targets. The accuracy of the scale determinations were verified by computing the actual size of a four door sedan and two station wagons used for ground transport. The measured and calculated lengths of the vehicles corresponded very well. In the case of the nighttime thermal images measured distances between roads were used for confirmation. Again the correspondance was excellent. The daytime photographic scale factors compared to thermal infrared night flights are:

Site 1	8-14 Infrared Thermal Image (night)	- 1:7600
	All Photographic Images (day)	- 1:3150
Site 2	8-14 Infrared Thermal Image (night)	- 1:8200
	All Photographic Images (day)	- 1:2800
Site 3	8-14 Infrared Thermal Image (night)	- 1:7600
	All Photographic Images (day)	- 1:2450

These scale factors show that aircraft altitude was maintained better during the infrared and microwave night missions than during the photographic day missions. This was probably due to high daytime wind velocities.

These scale factors were supplied to the computer and the microwave radiometric data was graphically printed out to match the individual scales. Therefore, all data is correlatable on a point-to-point basis.

Radiometer Data Reduction Procedure

RESOURCES TECHNOLOGY CORPORATION designed a procedure for the reduction and interpretation of ground brightness temperatures as detected by an airborne radiometer. The flights over oil pipelines resulted in automatically plotted profiles of brightness temperature against distance. Corrections for aircraft motion (pitch, roll, yaw) during flight are made and locations of intersection of radiometer antenna axis with the ground are accurately determined.

Inputs to the data reduction procedure consist of digital recordings of the aircraft flight dynamics on a one-half inch, seven-track digital tape which is computer compatible; a continuous magnetic field proportional to brightness temperatures on a one inch, fourteen-track, analog tape; and film strips from an airborne infrared scanner. Outputs are profiles of brightness temperature, resulting from data which has been numerically processed.

The equipment employed for entry into a general purpose digital computer, consists of the following instrumentations 1: Two Ampex 1900 tape recorder/play-back machines, Clevite chart recorder, 1400 Preston analog-to-digital converter and a Control Data Corporation 1700 computer. Photographs and infrared imagery are processed by photogrammetric methods as required.

There are three main computer programs involved in the data processing procedure, all coded in FORTRAN IV. One program accepts the digital one-half inch tape containing the aircraft history of flight motion parameters and produces a tape of angles, sines and cosines versus times. The second program accepts the radiometric data and produces a tape containing aircraft locations versus temperatures. The third program accepts the tapes produced by the first two programs and computes the radiometric antenna temperature as a function of antenna beam axis ground intercept. The details of the data reduction procedures are contained in Appendix A, Section VIII.

SECTION VI

DATA ANALYSIS AND INTERPRETATION

The basic techniques used to analyze and interpret the data were the same for all three pipeline sections. Primary to proper analysis and interpretation was correlation of the data in time and space.

The data for each of the three pipeline sections examined were mounted on a board such that point-to-point correlation was possible. Each data board has six strips of data, four obtained from cameras, one infrared scanner image and one set of microwave radiometer profiles. In each case the data are mounted in the same sequence. Starting from the top of the data board they are as follows:

- Color - Ektachrome MS Aerographic 2448
- RS-14 Infrared Image (night) 8-14μ
  3 milliradian resolution
- Black and White - Plux-X Aerographic 2402
- Black and White - Infrared Aerographic 2424
- Color - Ektachrome Infrared Aero 8443
- Microwave Profiles - Vertical and Horizontal (night)

All these data are very nearly the same scale for all three pipeline sections examined, with the exception of the RS-14 images which are about one half the scale of the photography and microwave profiles.

The basic premise derived from the theoretical modeling discussed previously is shown to be correct and valid by the obtained field data. That is, when a petroleum product pipeline leak is viewed with a microwave radiometer, there is an increase in microwave radiometric temperature values along with a decrease in the polarization contrast. The principle of detection is correct and the magnitude of the anomalies is about as expected for a 5^{o} beam system at 1000 feet. However, the polarization contrast ($\Delta T = T_V - T_H$) is much smaller than anticipated. The leak areas almost assume the characteristics of a microwave absorber. They appear to be very diffuse, with the horizontal and vertical temperature values being very nearly equal. This enhances detection capabilities and may greatly reduce false alarm rates. When the horizontal and vertical microwave profiles are coincident (observe the same target area), the polarization contrast is nearly zero, in

conjunction with an increase in microwave radiometric temperature, a petroleum product leak is present. These conditions are found to be true only when a petroleum leak was encountered.

Site Number One

Pipeline test site number 1 is located in southern Crane County. Five small leaks and one large leak occurred along the section of pipeline examined. The five small leaks were about 5-10 barrels and the large leak about 250-300 barrels. Most of the leaks occurred in 1968-69 and were one or more years old, except for a small 6 barrel leak which occurred in March of 1970.

Figure 19 is the pictorial and graphic data obtained from all the instruments flown. Surface and subsurface temperature data were gathered at all leak sites, but soil samples were obtained from only four leak areas. Since the thermal IR and microwave data shown in Figure 19 are from the night missions the ground data in Table 3 is also that obtained at night during the mission overflight. These nighttime temperature values show that the leak areas absorb more thermal energy than barren soil and the thermal inertia of the leak zone is higher than barren soil. This is more apparent when the daytime values (Table 4) are compared with those obtained at night. These two sets of data show that the thermal temperature of the leak zones are always higher than soil barren of oil. Insufficient data exists for an actual calculation of thermal diffusivity, but the data are sufficient to show the presence of oil does cause a decrease in electromagnetic albedo.

Photographic Imagery

All the leak zones are detectable with color photography, but they are not all detectable with black and white photography, black and white IR, or color IR. Even with color photography several of the smaller leaks (4, 5, 6) are barely discernible. This was the primary reason for selecting this site, the fact that leak size ranges from very small to very large.

It is interesting to note that along the pipeline right-of-way, those areas free of vegetation and where the sand is under dense (very loosely packed) the solar albedo is very high. This is apparent in both the visible and photographic IR. In this case the photographic flights were made at about 1300 hours and the solar angle was nearly vertical.

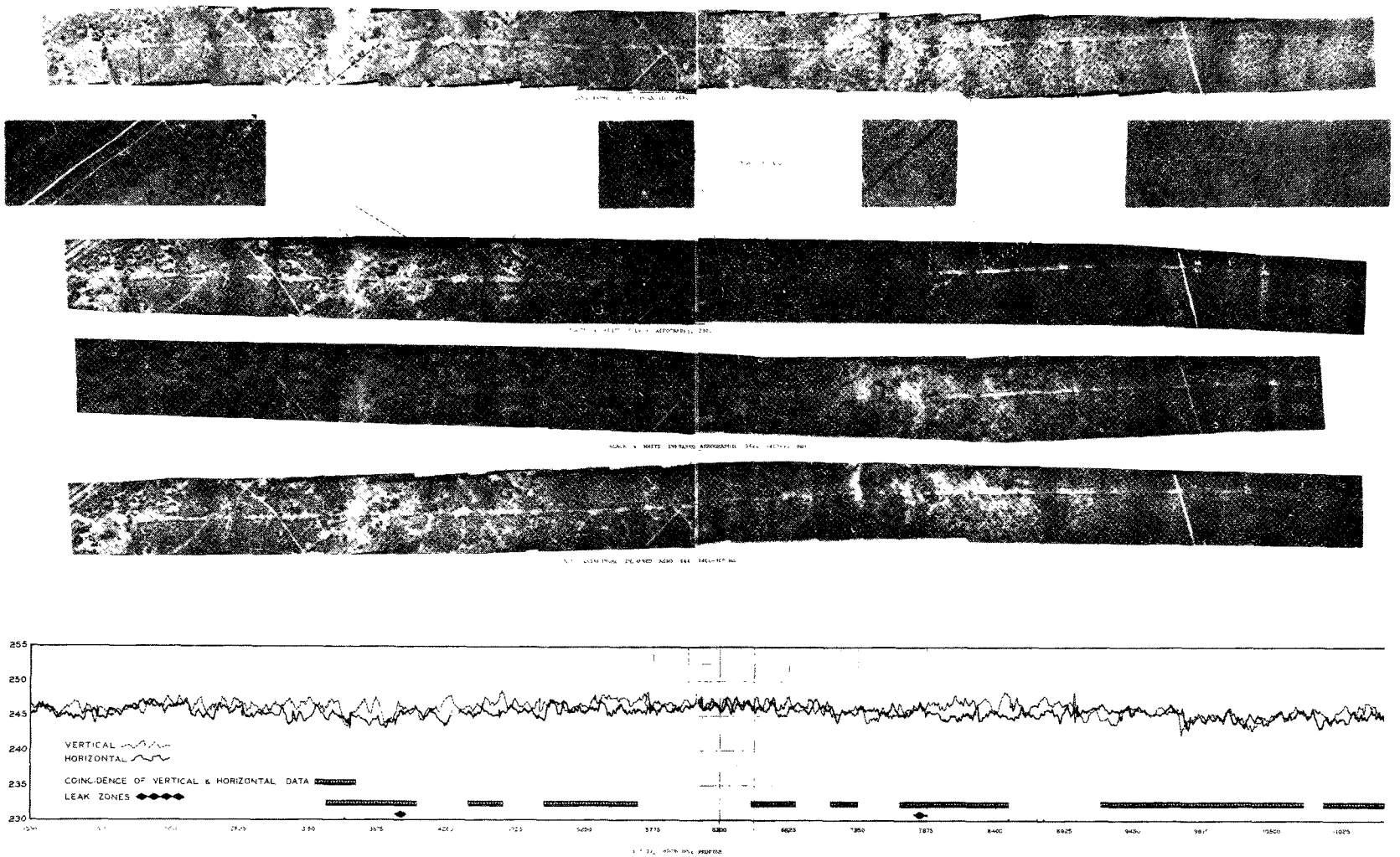

Figure 19 Multisensor Data Correlation, Site 1

PIPELINE SURVEY SITE NO. 1 (NIGHT)

Ground Crew: Shover & Brown

Leak Site	Time (local)	Surface Temp °C	Sub-Surface Temp °C	Surface Water %	Sub-Surface Water %	Surface Oil %	Sub-Surface Oil %	Comments
1	2245	25.0	30.0	-	-	-	-	Taken from oil zone (temperature only)
2	2250	27.0	33.5	-	-	-	-	Taken from oil zone (temperature only)
3	2300	25.0	30.0	0.5	0.9	0.0	0.0	Sample taken next to oil zone
		27.0	31.0	0.3	9.7	6.0	7.3	Sample taken from oil spill area
4	2300	25.0	29.5	0.4	0.6	0.1	0.0	Sample taken from sand next to spill
		26.0	32.1	0.3	0.1	2.8	2.5	Sample taken
5	2310	23.7	28.3	0.2	1.6	0.1	0.1	Soil sample obtained near leak area
		26.0	31.5	0.3	0.4	2.5	3.7	Soil sample obtained from leak area
6	2320	23.0	29.1	0.2	7.4	0.1	0.1	Soil sample near leak
		22.5	29.5	0.3	0.3	2.6	2.5	Sample from leak

SURFACE MEASUREMENTS, SITE NO. 1

Table 3

PIPELINE SURVEY SITE NO. 1 (DAY)

Ground Crew: Shover & Brown

Leak Site	Time (local)	Surface Temp °C	Sub-Surface Temp °C	Surface Water %	Sub-Surface Water %	Surface Oil %	Sub-Surface Oil %	Comments
1	1430	46.0	28.8	-	-	-	-	Taken from oil zone
2	1433	45.0	32.0	-	-	-	-	Taken from oil zone
3	1440	42.0	28.5	0.5	0.9	0.0	0.0	Taken from soil
	1444	46.2	31.0	0.3	9.7	6.0	7.3	Taken from oil zone
4	1330	40.0	28.0	0.4	0.6	0.1	0.0	Taken from soil
	1340	48.0	32.0	0.3	0.1	2.8	2.5	Taken from oil zone
5	1210	34.0	26.5	0.2	1.6	0.1	0.1	Taken from soil
	1210	39.0	28.2	0.3	0.4	2.5	3.7	Taken from oil zone
6	1240	33.0	27.5	0.2	7.4	0.1	0.1	Taken from soil
	1232	40.8	28.2	0.3	0.3	2.6	2.5	Taken from oil zone

* All water and oil saturation data for both day and night are taken from daytime samples. Saturations were assumed not to change significantly in the 10 hour period between temperature measurement.

SURFACE MEASUREMENTS, SITE NO. 1

Table 4

The only photographic sensor that could be used to document the occurance of a leak along this section of pipeline was color photography.

It should also be pointed out, that even in this topographically flat country, oil flows away from the pipeline following topographic features. Higher slope angles would result in larger areas of contamination and very probably stream contamination. The source of such contamination would be almost impossible to identify visually, in areas with topographic relief and vegetation cover.

Infrared Imagery

The 8-14 micron infrared imagery was obtained at 0230 hours on 12 June 1970 simultaneously with microwave radiometer (13.7 GHz) data. The ground data show that the thermal temperatures of the leak zones are always (day and night) higher than the adjacent soil. This should make the oil stain areas appear warmer than the surrounding soil.

An interesting phenomenon occurs in the infrared imagery. The active area, or area of highest saturation, causes a warm anomaly. However, the surrounding "scar" or "oil trail" area which consists primarily of dead oil, in more or less solid or plastic state, appears cool in the infrared. Measured thermal temperatures in these regions of dead oil do not indicate a cool anomaly should exist. Therefore, it must be a change in the emissivity function which makes these areas appear cool in the infrared. Temperature anomalies associated with vegetation and exposed pipe, among other things, have equal or larger IR temperatures. This results in a high false alarm rate under the conditions encountered. It would be extremely difficult to identify particular leaks using only thermal infrared imagery. However, the pipeline right-of-ways are easily idenfified by thermal IR. This imagery shows, quite well, a number of other pipelines crossing the main trunk line. These crossing lines are part of the gathering system associated with a nearby oil field.

Microwave Radiometric Profiles

Two separate day and two separate night flights were made so that both vertical and horizontal polarized microwave profiles could be obtained for day and night conditions. The two profiles displayed in Figure 19 are those obtained during the night flights. Ground track coincidence of the two profiles

occurred less than 60% of the time, and even then, exact beam coincidence was probably less than 20%. This problem is discussed under Problem Areas, Section V.

Almost all of the leaks, except the one at 7820 feet, were too small to affect very large changes in the microwave temperature. This is because of the 5^{0} beam diameter of the microwave antenna. With a look angle of approximately 35^{0} at 1000 feet altitude the beam diameter for the ground intercept would be about 140 feet or an area of 16,000 ft. As shown in the theoretical section, this would amount to microwave anomalies of less than $2^{0}K$ for the leaks at 3388 feet (6), 3831 feet (5), 8504 feet (3), 8689 feet (2), and 8745 feet (1). Therefore, the only anomaly available for microwave analysis is that occurring at 7820 feet (4).

The average microwave background temperature in the region of leak No. 4 is $245^{0}K$ which results in an emissivity (ε) of 0.80, using the simplified expression:

$$T_A = \varepsilon T_g + (1 - \varepsilon) T_S$$

and 0.81 for the oil leak zone.

The most interesting feature associated with this leak is the fact that the polarization contrast ($\Delta T = T_V - T_H$) does to zero. That is both the horizontal and vertical microwave temperatures are a measured $247^{0}K$. This means that oil leak zones behave like diffuse materials and the reduction in polarization differential predicted theoretically is greater than expected.

A great deal of bulldozer activity has been conducted in the area of leak #4 in an effort to cover the saturated soil. This is done to keep local cattle from developing sore feet and possi bly suffering permanent injury. Even with thick cover (8 - 12 inches) the leak area is apparent in the microwave profile.

Site Number Two

Pipeline test site number 2 is located about 2 miles southeast of Wink, Texas. Six relatively large leaks were visible along the stretch of pipeline examined. These leaks ranged in size classification from 500 barrels to 30 barrels and stained the surface.

Figure 20 is the pictorial and graphic data obtained from all the remote sensors including photography. Starting from the left and using the footage markers along the base of the microwave temperature profile the visible leaks are: Number 1 -

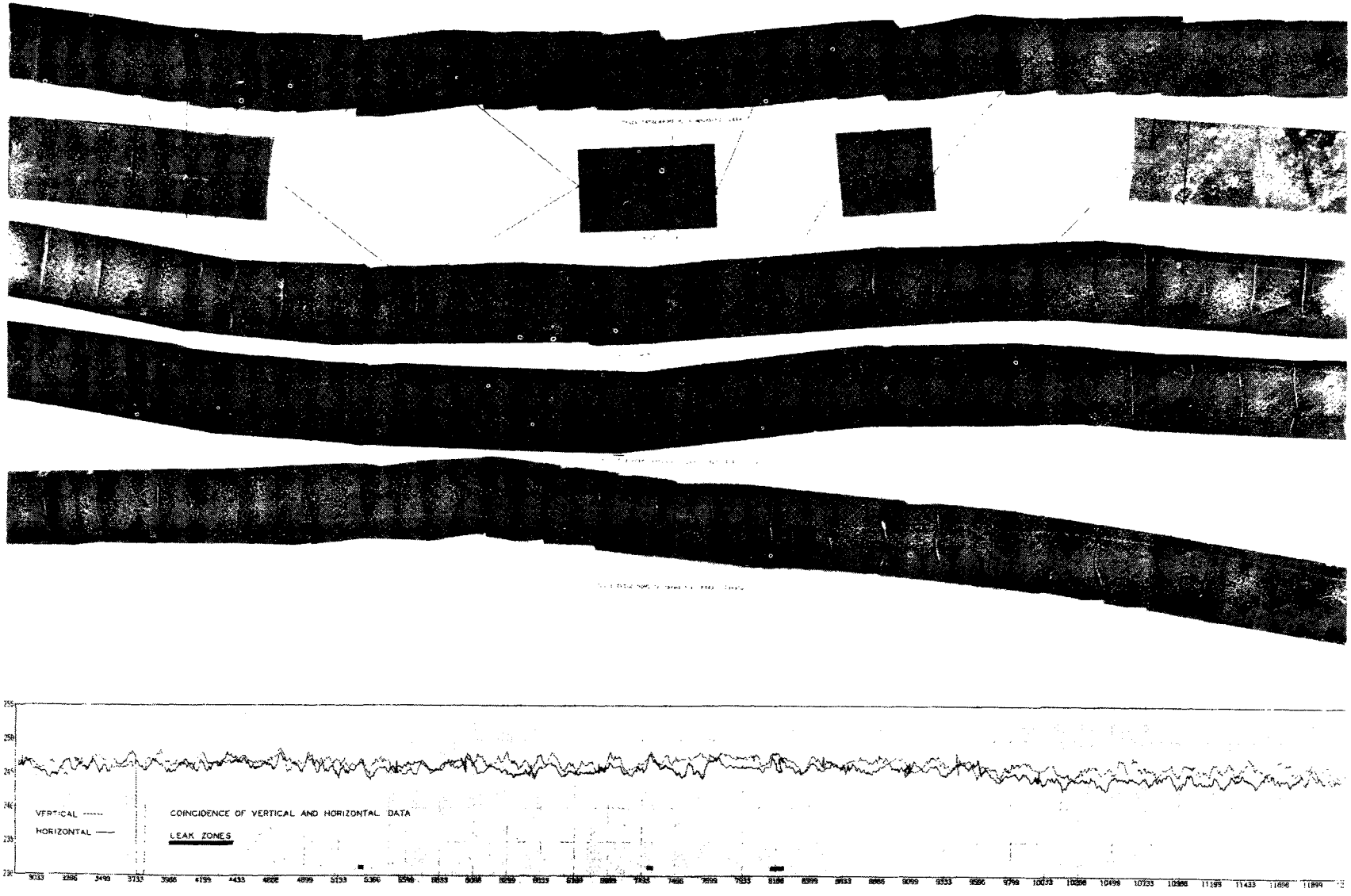

Figure 20 Multisensor Data Correlation, Site 2

3499 feet, Number 2 - 4120 feet, Number 3 - 4540 feet, Number 4 - 7285 feet, Number 5 - 8350 feet and Number 6 centered at 8920 feet. Of these leaks, leak Number 4 - 7285 feet was encountered by both the horizontal and vertical microwave beams. All visible leak areas are identifiable to some degree by color photography, infrared imagery (8-14μ), black and white photography, black and white infrared and color infrared. However, there are two leaks, one at 5300 feet and one at 8166 feet, that were discovered after reduction of the microwave radiometer data and closer inspection of the color photography.

The leak at 5300 feet is slightly visible in the color photography and even here only very slight light brown staining is visible on very close and detailed inspection. The ground crew, which inspected the entire measured pipeline section, did not notice this leak area even though they walked over it several times. No ground correlation data were obtained so saturation and ground temperature data are not available. The leak area at 8166 feet is evident on all the imagery, but very weak in the thermal IR.

Photographic Imagery

All the leak zones were detected with all the photographic sensors with the exception of the leak at 5300 feet which was only visible with color photography. Listing the photographic sensors in their order of "best for detection", they are:

- Color Photography - Aerographic 2448
- Color Infrared - Aero 8443
- Black and White - Plus X Aerographic 2402
- Black and White Infrared - Aerographic 2424

An interesting side issue is the very obvious change in vegetation color beginning at about 9799 feet. To the left (south) the vegetation is light green and sparse compared to the area north of 9799 feet. This is only obvious in the color photography among the imaging instruments. However, there is very obvious changes in the microwave radiometric profile data. The microwave radiometric base temperature drops about two degrees and the polarization differential very obviously increases. This change will be more thoroughly discussed under microwave radiometry.

Infrared Imagery

The 8-14 micron infrared imagery was obtained at night (0300 hours, 12 June 1970) simultaneously with the microwave radiometric profiles. In support of both the infrared and microwave data, the ground correlation data were gathered (Table 5).

In all cases the nighttime thermometer temperatures measured within the areas saturated with oil, both surface and subsurface (10 inches), were higher than those temperatures measured in unsaturated areas. The one exception is the surface temperatures measured "on" and "off" the leak at 8920 feet. In this case identical surface temperatures were recorded. These temperature differentials are evident in the infrared imagery and certainly the leak areas where thermal temperatures were measured show up as bright regions. The indication is that the dark (visual) oil saturated ground has a higher thermal inertia than unsaturated ground. This becomes evident when the daytime thermal measurements (Table 6) are compared with the night measurements.

The surface temperature of the oil free area has an average of about 45.0°C during the day and only 20.1°C at night. A drop of about 23.8°C occurs for the unsaturated area. However, the surface temperatures of the leak areas average about 45.4°C during the day and 22.8°C during the night. This drop of 22.6°C, shows characteristically higher thermal inertia for fluid saturated soils. This is evident in the IR imagery and the oil saturated soils are warm compared to the surrounding soil. However, the cool halo observed in site 1 imagery also exists around site 2 leaks.

Leak site Number 4 (7285 feet) was bulldozed over. That is, the oil was covered up by scraping dirt from the surrounding area over the oil area. The dozed area appears cool as compared to both the undistrubed soil and those oil saturated areas that were not quite covered. In this regard it acts much the same as the road adjacent to the pipeline. This cooling is due to the rapid loss of heat from the smoother, unvegetated bulldozed area.

All of the leak areas which produce surface staining are visible to the infrared imager as warm anomalous spots along what is normally a cool track created by the pipeline or the surface scar of the pipeline. It is difficult to tell from this pipeline right-of-way which is creating the cool anomaly, the scar or cooling due to some other effect associated with pipeline presence. The subsurface temperature (10") is close to 90°F which is probably warmer than the oil in the line itself and some heat is most likely transferred from the ground to

PIPELINE SURVEY SITE NO. 2 (NIGHT)

Ground Crew: Kennedy & Shows

Leak Site	Time (local)	Surface Temp ^{o}C	Sub-Surface Temp ^{o}C	Surface Water %	Sub-Surface Water %	Surface Oil %	Sub-Surface Oil %	Comments
4120 ft. (No. 2)	0340	19.5	29.8	0.9	2.1	0.1	0.1	Sample taken 75'SE of leak center (no oil)
	0350	23.4	32.5	1.0	13.6	17.5	6.0	Sample taken from center of visible leak area
4540 ft. (No. 3)	0330	19.0	30.0	1.4	2.5	0.0	0.0	Sample taken 75 E of leak center
	0336	20.2	31.6	1.0	13.0	18.8	9.0	Sample taken from center of visible leak
7285 ft. (No. 4)	0315	19.4	29.8	1.9	5.1	0.1	0.2	Sample taken 75'W of leak center
	0310	25.0	31.2	5.1	20.9	10.2	4.8	Sample taken from directly over pipe-line
8920 ft. (No. 6)	0300	22.5	29.5	0.7	1.9	0.0	0.0	Sample taken 75'W of leak center
	0308	22.5	31.0	1.6	10.2	27.6	6.9	Sample taken from center of visible leak area

SURFACE MEASUREMENTS, SITE # 2

Table 5

PIPELINE SURVEY SITE NO. 2 (DAY)

Ground Crew: Kennedy & Shows

Leak Site	Time (local)	Surface Temp ^{o}C	Sub-Surface Temp ^{o}C	Surface Water %	Sub-Surface Water %	Surface Oil %	Sub-Surface Oil %	Comments
4120 ft. (No. 2)	1305	47.5	29.0	0.8	2.2	0.0	0.1	Sample taken 75 SE of leak center
	1310	46.5	33.0	1.1	13.6	18.0	6.2	Sample taken from center of leak area
4540 ft. (No. 3)	1320	45.2	30.0	1.2	2.2	0.1	0.1	Sample taken 75 E of leak center
	1330	46.2	32.2	0.8	9.0	16.2	9.4	Sample taken at leak center
7285 ft. (No. 4)	1438	40.0	32.5	-	-	-	-	In soil area) No
	1447	44.5	36.0	-	-	-	-	In oil zone) samples
8920 ft. (No. 6)	1418	43.0	31.0	-	-	-	-	In soil area) No
	1425	44.5	31.5	-	-	-	-	In oil zone) samples

SURFACE MEASUREMENTS, SITE NO. 2

Table 6

the pipeline causing secondary effects that are detectable at the surface.

Microwave Radiometric Profiles

The microwave radiometric profiles, one vertically polarized and one horizontally polarized, were obtained on two separate daylight flights separated by about 10 minutes and two separate night flights separated by about 10 minutes. The two profiles displayed in Figure 20 are those obtained during the night missions. The major problem areas, discussed later, were maintaining a beam intercept of the pipeline along its entire length and coincident of the horizontal and vertical profiles flown at two separate times. Only short disconnected sections of the pipeline have coincident data.

If the apparent microwave brightness temperature is averaged from 3966 feet to 9799 feet (Figure 20) a temperature of about 246.5°K is realized. Using the simple formula for estimating emissivity, $T_A = \varepsilon T_g + (1 - \varepsilon) T_S$, where:

T_A = Apparent microwave temperature

ε = Microwave emissivity

T_g = Thermal ground temperature

T_S = Microwave sky temperature

the microwave emissivity is about 0.83, which is very nearly the theoretical value for a look angle of 35°, ground temperature of 293°K, and a sky temperature of about 20°K. Also the vertical polarized value is slightly greater than the horizontal polarized values, which is necessarily true both empirically and theoretically. From 9799 feet to the end of the flight line the vertical temperature remains at an average temperature of 246.5°K but the horizontal temperature drops to 244°K, a decrease of 2.5°K. These conditions, a decrease in horizontal temperature and an increase in polarization differential are generally caused by increased moisture content. In this case the increase in moisture content is supported by a definite change in vegetation color. A decrease of 2.4°K means an increase of about 3% in soil moisture content (Kennedy 1967). In this arid west Texas area this is more than sufficient to increase vegetation vigor.

Three leak zones were encountered and traversed by both the horizontal and vertical beams. Two leaks are obvious and one is not truly visible at the surface. However, once it was

identified by microwave profile data, some slight staining was found on the color photography. These three leaks represent a nice spectrum of leak occurrances. Beginning at the right in Figure 20 and moving to the left, the leak at 8166 feet is relatively new, and was not visible at the surface, but is evident from the air. The next leak at 7285 feet is old (1968), has been partially covered by bulldozing, and is primarily visible because of the large land scar. The third leak, yet to be identified as a leak circumstance, is not visible on the ground or from the air, but only by microwave observation. It may be a false alarm but the indications are that a leak does exist.

A comparison of the measured data with the original theoretical predications show relatively close agreement. In this case the closest theoretical values are those calculated for 10% water and 10% oil in a sandy loam soil at 25°C. Allowances must be made for the cooling effects of increased fluid content, decrease in thermal temperature and temperature increase due to surface roughness. The water content is a measured 21%, 11% higher than that used in theory, and the thermal temperature (night) is a measured 20°C as opposed to 25°C used in the theoretical predictions. These would result in a decrease in microwave temperature of about 22°K, or reduce the theoretical prediction for horizontal polarization of 270° to about 248°K for the oil spill areas. The roughness of the surface would increase the apparent temperature somewhat, but this increase is difficult to estimate.

It should also be mentioned that the beam diameter of the very low resolution system was about 140 feet at the ground (5° beam, viewing angle 35° at 1000 feet altitude). This means that the encountered leak zone did not fill the entire beam. Therefore, the microwave thermal anomalies created by the addition of oil to the native soil are increases superimposed on normal values. For instance the leak at 7285 feet only occupied 56% of the beam area. Therefore, a microwave temperature increase of 10 degrees would show up as a 5 degree increase. The leak at 8166 feet occupied only 34% of the beam area and a 10° microwave anomaly would be about 3.4°. Higher resolution systems would represent a significant increase in ability to detect leak areas. All three leak areas encountered along pipeline section #2 have anomalies of the proper magnitude.

Site Number Three

Test site Number 3 is located above five miles east of Wink, Texas. Six relatively large leaks are visible along the one and one quarter mile section of line selected for examination.

The most conspicuous leak centered at 8932 feet was over 1000 barrels and occurred at the junction of two trunk lines. These leaks follow the same pattern as found in the other two sites. That is, best detection is by color photography followed by color infrared, infrared imagery, black and white photography and black and white infrared, in the order presented. This is especially evident in Figure 21 which shows the data arranged in the same order as the previous sites.

The correlation of pipeline leak data in the infrared and microwave portions of the spectra is not possible for this particular site because the ground track of the microwave radiometer is centered about 300 feet south of the pipeline right-of-way. Although the microwave radiometer ground track did impinge the pipeline in some cases, neither a ground station location nor a leak were encountered simultaneously. This was due to the pilot's inability to judge ground intercept with aircraft flight track and is discussed under Section VI, Problem Areas. In the case of Site No. 3, it was a case of over compensation for wind.

Also, difficulties with the ground vehicle during the night overflight prevented obtaining ground information. Therefore, further analysis of the data is unwarranted.

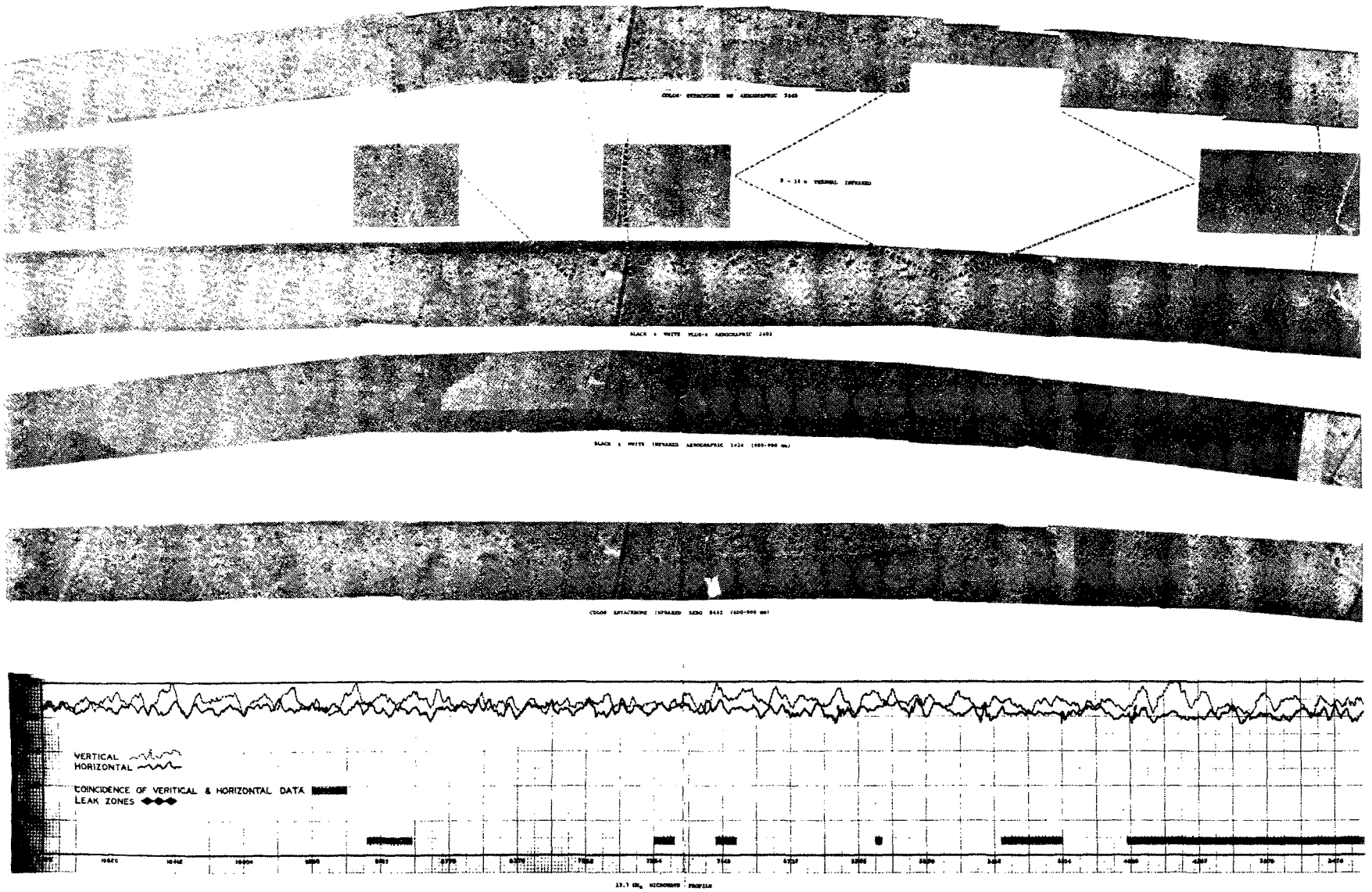

Figure 21 Multisensor Data Correlation, Site 3

SECTION VII

PROBLEM AREAS AND SOLUTIONS

Most of the problem areas encountered in the performance of this project were discovered during the data reduction phase and are primarily mechanical.

Pilot Judgment

The predominant problem can be identified as pilot judgment. If, as in this project, there is a requirement to fly the same ground track several times such that the instruments sense the same areas several times, a critical problem of visual alignment is apparent. The ability to fly the same surface track is made more difficult if the instruments view the ground at an angle off the vertical and during periods of high gusty winds. High winds, approximately 30 knots due east at ground level, were especially troublesome during the daytime flights. This is apparent from the aircraft shadow which is visible on the photography. During the night flights ground level winds were "dead-still".

The pilot visually aligns the nose of the aircraft with the ground markers for a continuous line of sight track. However, if the aircraft is "crabbed" into the wind the alignment geometrically offsets the aircraft path in the direction in which the wind is blowing. This is graphically shown in Figure 22. When the measuring instrument points aft, as was the case, the problem is amplified and the actual ground track is further displaced in the direction in which the wind is blowing. Certainly the pilot cannot pre-judge the offsets involved and make the necessary corrections by performing mental gymnastics.

Since the instrument is fixed, that is, hard mounted to the aircraft frame, it appears that the best solution is to fly a series of lines offset from each other in the direction from which the wind is blowing. The distance to offset can be "guessed at" by observing the drift angle obtained from the doppler navigator. It may be necessary to develop some simple nomographs which show the expected offset as functions of wind velocity, wind direction and altitude. This would increase the probability of a proper or usable ground track, but will not eliminate the necessity of flying the same general line at least three or four times with progressive offsets in the direction from which the wind is blowing. Of course this problem is completely eliminated if microwave imaging systems were used.

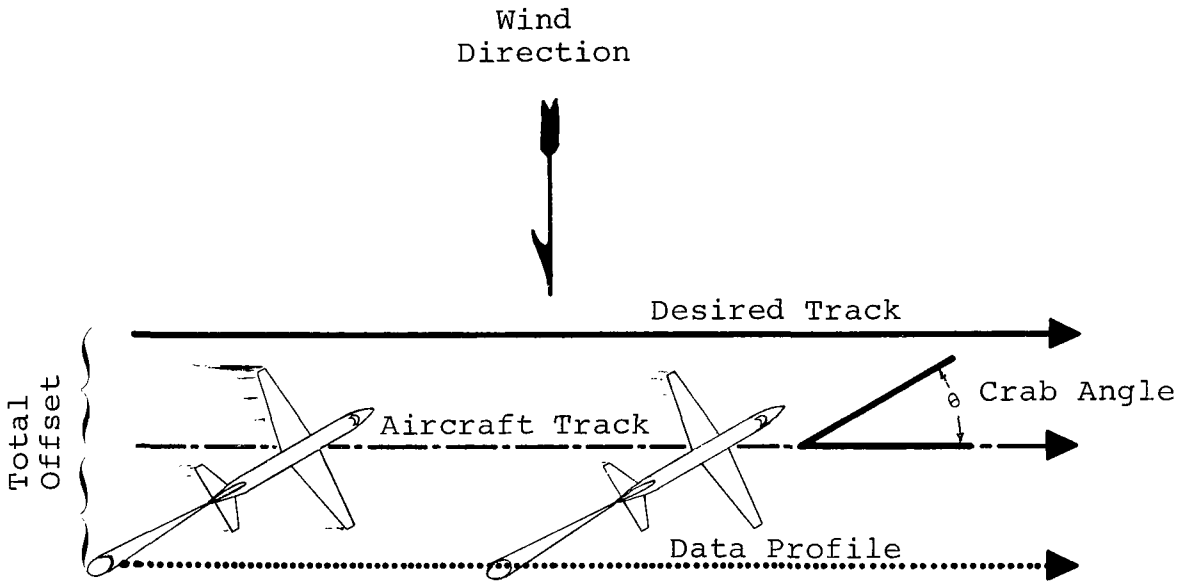

Figure 22 Profile Offset Due to Wind

Aircraft Dynamics

In addition to the tracking error mentioned above, aircraft dynamics pitch, roll, yaw and velocity changes also cause deviations from the desired ground track because the measuring instruments are hard mounted. All of these parameters are continuously recorded on magnetic tape during the data runs and are correlated with all other data using the 400 Hz signal discussed in a previous report. These data are inputs to the computer data reduction program and the entire flight line is corrected to display the actual ground track from which data is obtained. However, knowing that the problem exists and performing error free corrections does not make target acquisition any more accurate. This is after the fact information and only informative in that it determines whether or not the sensor beams passed over the desired area. In this particular case, the identified and marked pipeline leak sites. Since realtime data reduction in the aircraft is impractical, the solution to this problem is to increase the number of over-passes to be relatively certain that the leak areas were indeed observed. Of course, in an operational system a multibeam system of sufficient path width would be used to insure observation. However, in the case of a research project where a single beam system is used multiple flights are required.

The actual ground tracks of microwave radiometer data acquired during performance of this field project are shown in Figures 23, 24, and 25.

Polarization Differential

The computer simulation program which initiated this project, predicted that when a microwave radiometer observed a leak circumstance the microwave temperature would increase and the polarization contrast ($\Delta T = T_V - T_h$) would decrease. This determination was based on the assumption that the horizontal and vertical target areas were exactly the same. As explained earlier, exact coincidence is rather rare for a system which does not measure both components simultaneously and redundant flights are required. However, when partial coincidence occurs, that is major parts of observing beams cover the same area, and an oil leak is present the polarization contrast should decrease significantly along with temperature increases for both the horizontal and vertical microwave antenna temperatures. This was found to be true in almost every case of coincident leak observations. However, it is possible that non-coincident portions of the observed areas could contain objects which cause

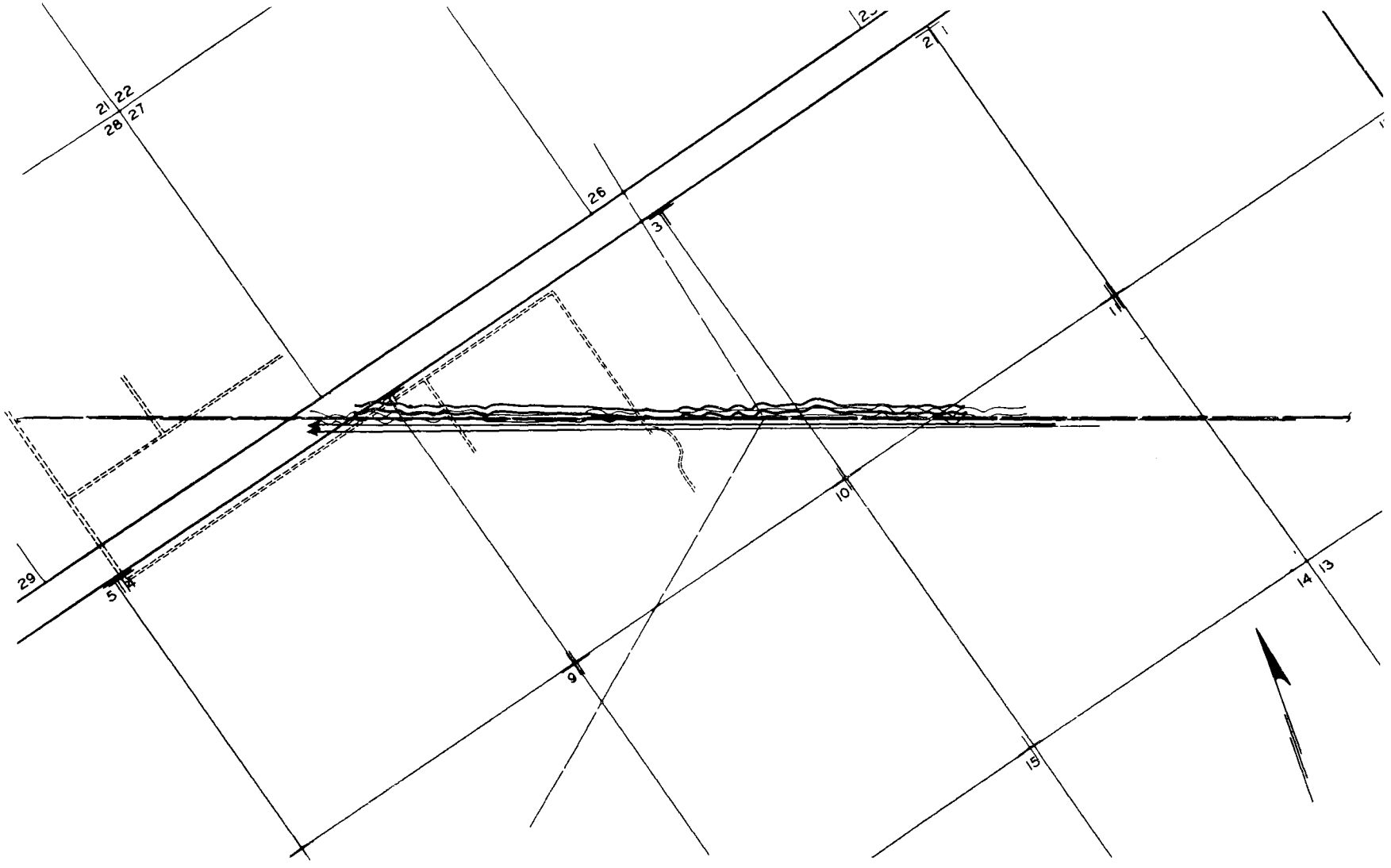

Figure 23 Profile Ground Track, Site 1

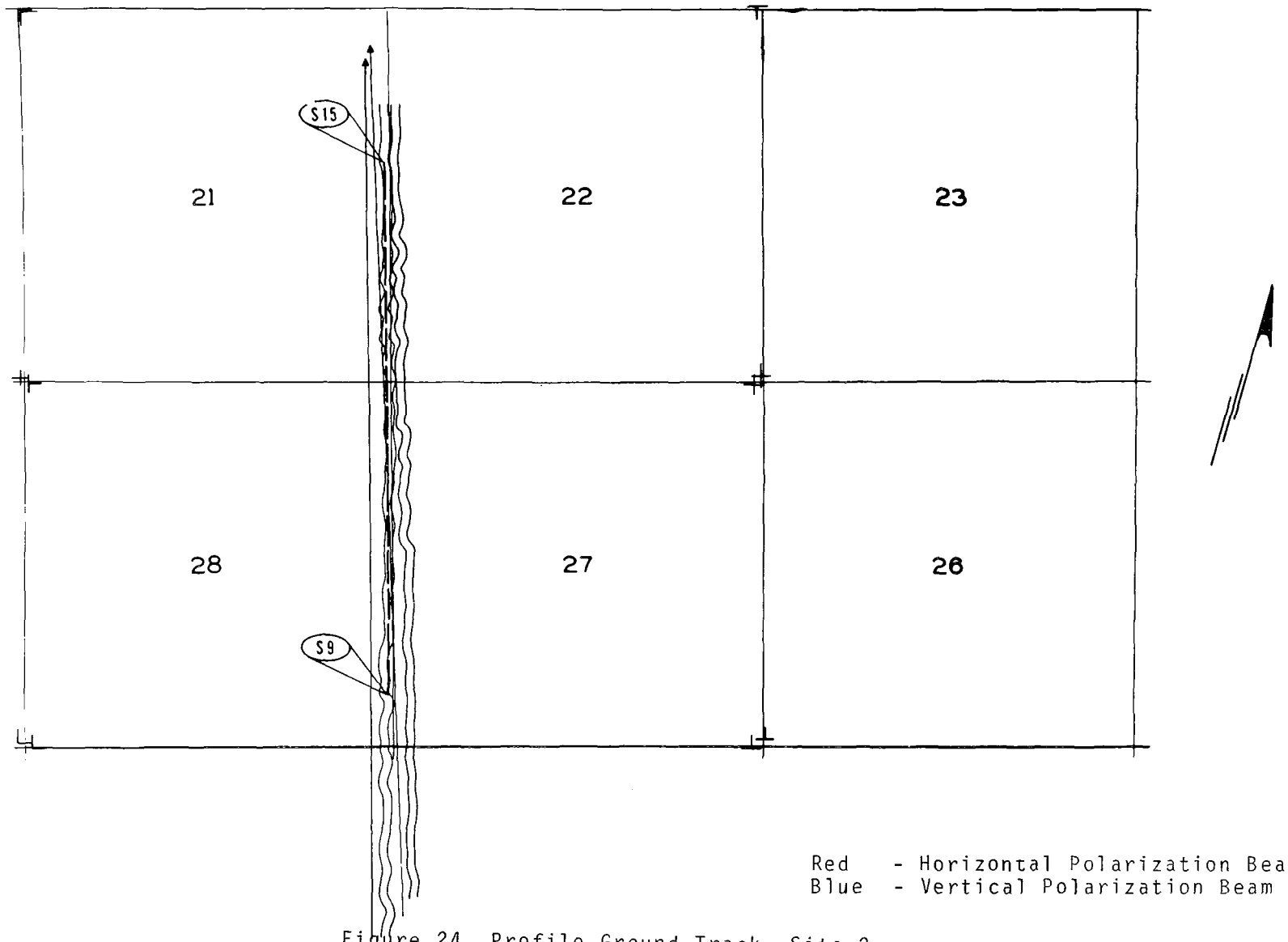

Red - Horizontal Polarization Beam
Blue - Vertical Polarization Beam

Figure 24 Profile Ground Track, Site 2

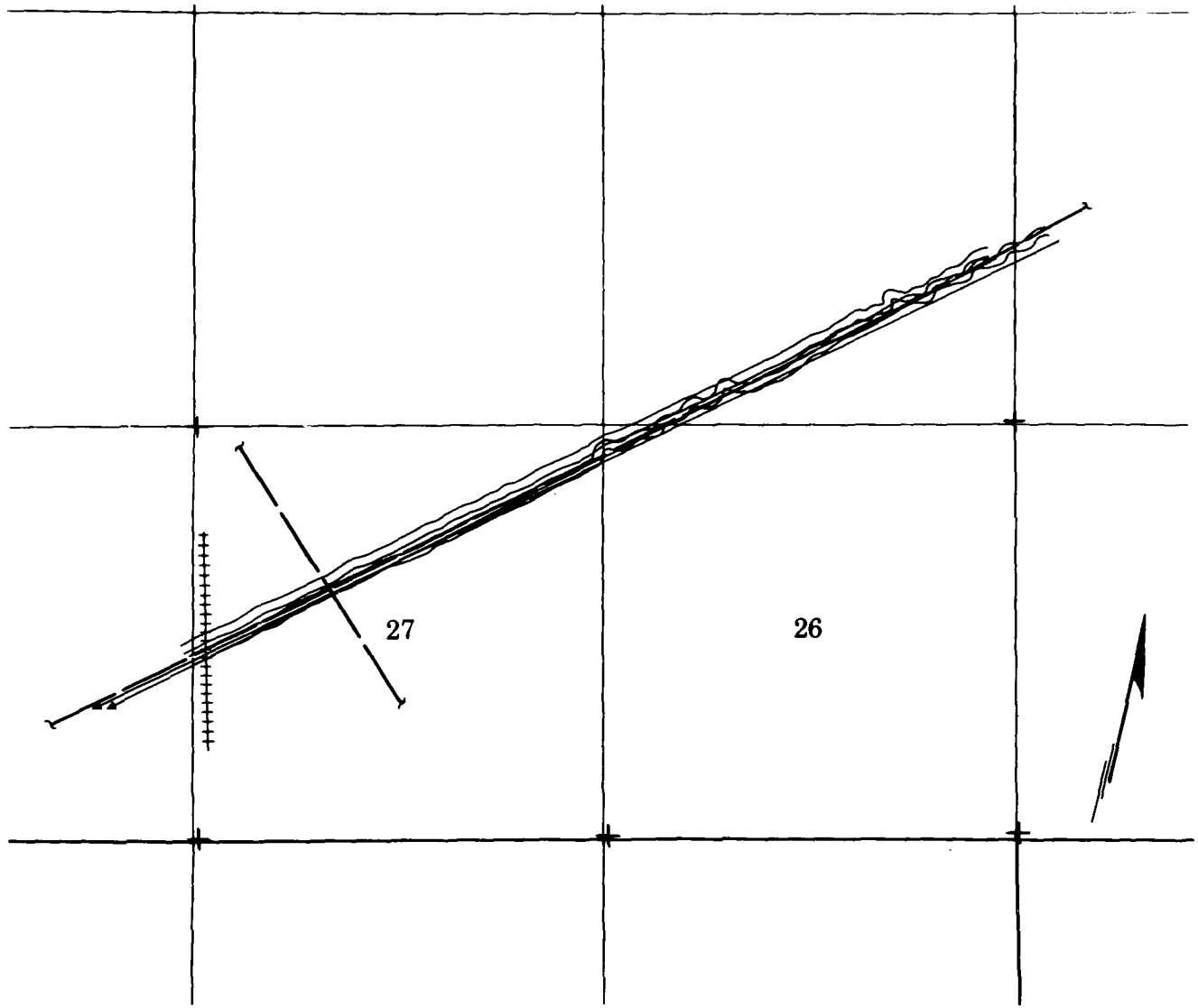

Red - Horizontal Polarization Beam
Blue - Vertical Polarization Beam

Figure 25 Profile Ground Track, Site 3

an increase in polarization contrast and even make one or the other polarized components tend to be cooler. In this case a leak would be passed over and not detected. While this problem was apparently not encountered in this program it should be considered in future projects.

The obvious solution is to always take data using a dual polarized microwave radiometer system, which simultaneously obtains both horizontal and vertical data.

SECTION VIII

APPENDIX A

RADIOMETER DATA REDUCTION PROCEDURES

Flight Dynamics Parameters

In order to correlate brightness temperatures with ground location, a time profile of the airplane's position and its angles of roll, pitch and yaw is required. The angle data are provided by an Incredata recording system. This system accepts voltages from the aircraft motion systems, such as the doppler navigator, magnetic compass, etc., and digitizes the information, which is stored in binary on a seven-track tape, with odd parity. The system accepts an aircraft clock output and at the beginning of each record the time of day is recorded in hours, minutes and seconds to an accuracy ± .001 seconds. When the system is first turned on, values of twelve thumbwheel settings are first written on the tape in binary-coded decimal format, odd parity. The thumbwheels are manually set to values which identify the month, day, site number, flight line number, the number of the pass over the flight line, and whether the flight is day or night.

At the end of a mission an Incredata tape is available which contains thumbwheel settings identifying the data to follow, time of day, and the angles of roll, pitch and yaw at 400 millisecond intervals.

The first two words of every record on the tape are printed to obtain thumbwheel settings, to count records and to locate end-of-files, if any. This information is needed for input to a computer program which sorts the data, unpacks the binary representation and forms FORTRAN word representation. If more than one input Incredata tape was required it also merges the tapes. Finally, from the calibration curves of voltage versus angle and the binary word length versus voltage limits, the data are converted to tables of roll, pitch and yaw in radians versus time of day.

The tape representation at the top of Figure 26 shows thumbwheel record followed by a number of DATA records. Between records there is a 1-inch unrecorded area denoted IRG (interrecord gap).

A thumbwheel block contains 12 characters which are set shortly before beginning a flight line. The 12 characters, from left to right, are in binary coded decimal and having the following meanings:

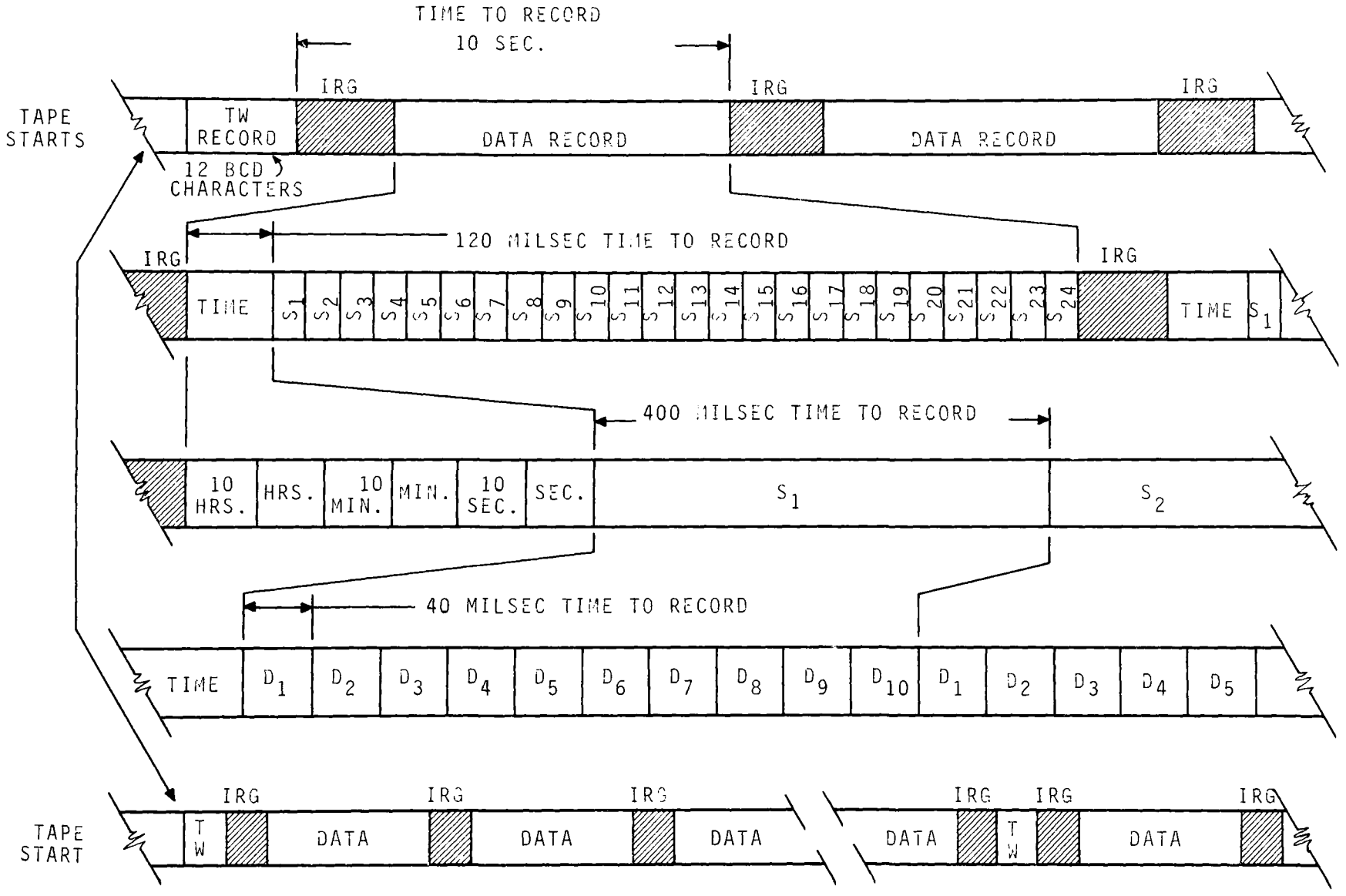

Figure 26 Schematic of Incredata Tape

Character	Meaning
1	10's of months
2	units of months
3	10's of days
4	units of days
5	not used
6	site number, even 10's digit
7	site number, units digit
8	flight line number, even 10's digit
9	flight line number, units digit
10	refly* number, even 10's digit
11	refly number, units digit
12	day flight = 4, night flight = 8

The first four tape tracks record the values in binary, the next two tracks are blanks, and the seventh track is employed for parity.

The second tape representation of Figure 26 is an expansion of a DATA record block. The six left-most tape frames are in the same binary coded decimal format as is the TW record and contain the time. This is clock time and although only shown to one second in significant figures, it is actually accurate to one millisecond.

Following the time there are 24 sets of parameter values, in the figure denoted S_1, S_2 ..... D_{10}. The D's are two-character, 11-binary-digit numbers which are the values of flight

---

* Refly number refers to how many times a line was flown before successful data collecting occurred.

dynamics parameters, as follows:

D_1 = ground speed

D_2 = drift angle

D_3 = miles to go along track

D_4 = not used

D_5 = magnetic heading

D_6 = pitch

D_7 = roll

D_8 = course altitude

D_9 = fine altitude

D_{10} = signal ground

To convert angles from digital counts to radians, calibration curves are used. These curves relate voltage to angle, and angle to counts. The range of 0 to 5 volts is digitized into a register of eleven bits, that is, a range of 0 to $2^{11} - 1 - 2047$. This yields a conversion factor:

2047 counts = 5 volts

The pitch calibration provided the following voltage-to-angle relationships:

2.72 volts = 20^o, nose up

2.15 volts = 20^o, nose down

from which the pitch is given in radians by the equation

$$\beta = 2.982368 - .002991677D$$

where D is in counts, and β to pitch.

The roll calibration yields

2.61 volts = 20^o, right wing down

2.04 volts = 20^o, right wing up

from which the algorithm for roll (α) is derived:

$$\alpha = -2.847641 + .002991677D$$

again D in counts, α in radians.

The magnetic heading calibration yields the set

$$0 \text{ volts} = 20^{o} \text{ azimuth}$$

$$5 \text{ volts} = 370^{o} \text{ azimuth}$$

from which the equation to compute magnetic heading, H", is determined

$$H" = 20 + .1709819D \text{ (degrees)}$$

Denoting the magnetic declination ΔH, the true heading, H, is given by

$$H = H" + \Delta H, \text{ modulus } 360 \text{ (degrees)}$$

from which the yaw, can be calculated using

$$\gamma = .017453293 (H' - H) \quad \text{(radians)}$$

where H' is the azimuth of the flight line.

The computer subroutine which makes these conversions from counts to angles also determines the times associated with each angle.

A ground-track coordinate system is required for remote sensor system ground intercepts and is defined as follows: The X-axis is horizontal and coincides with the flight line, positive in the direction of flight; the Z-axis is vertical, positive upwards; the Y-axis is that required to form a right-handed coordinate system. This, the ground track system and the aircraft-fixed system, Figure 27, coincide when roll, pitch and yaw equal zero.

The aircraft attitude measuring system is mechanized such that roll, pitch and yaw may be considered unordered, simultaneous rotations. Furthermore, careful operation during the flight constrains these to be small angles so that infinitesimal rotation theory may be utilized in data reduction. Accordingly, the transformation of the unit vector along the sensor beam axis from aircraft-fixed coordinates to ground track coordinates is performed with the following equations:

$$Q_1 = P_1 - \gamma P_2 + \beta P_3$$

$$Q_2 = \gamma P_1 + P_2 - \alpha P_3$$

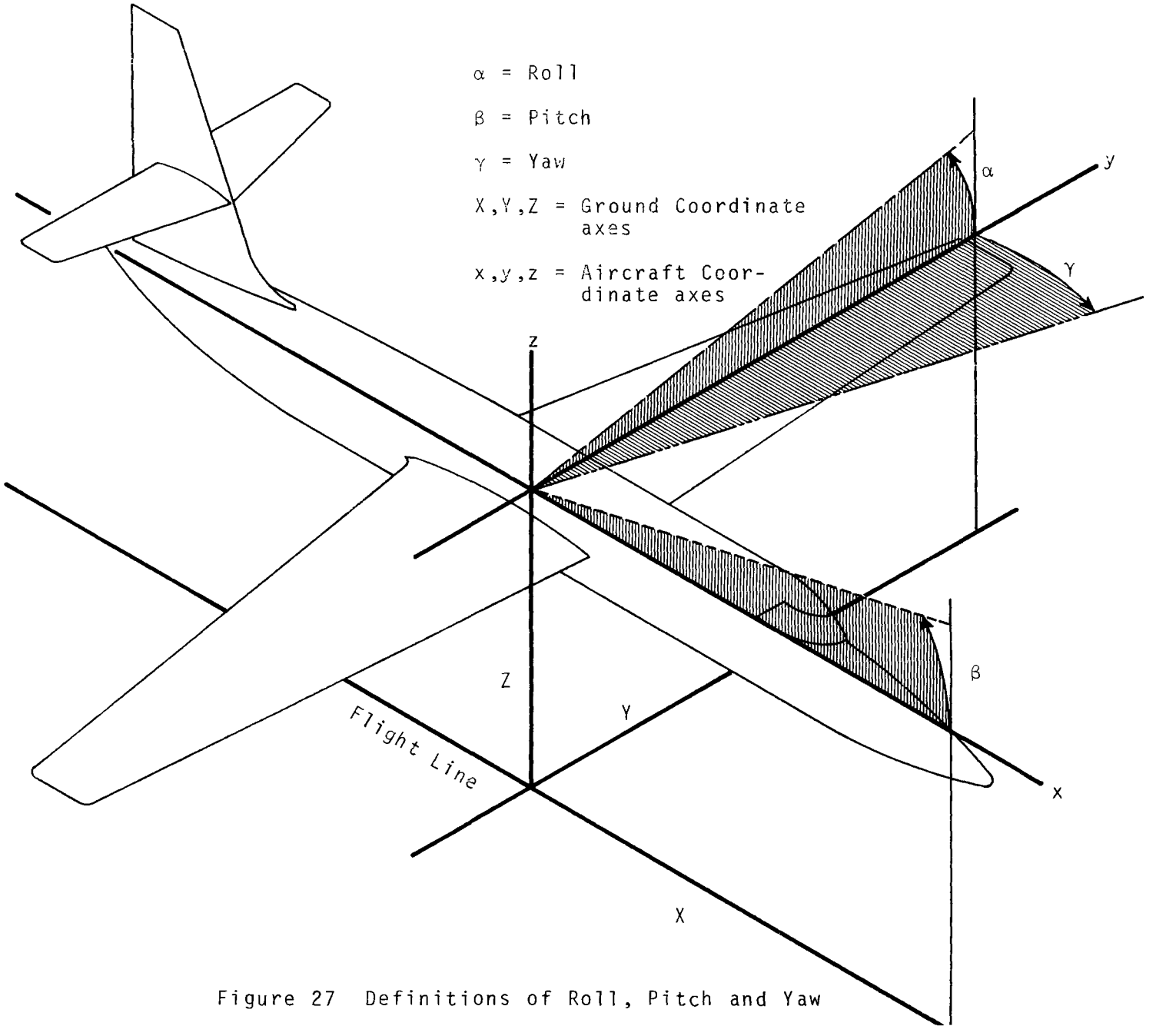

Figure 27 Definitions of Roll, Pitch and Yaw

$$Q_3 = \beta P_1 + \alpha P_2 + P_3$$

where $(P_1, P_2, P_3)^T$ and $(Q_1, Q_2, Q_3)^T$ are the X, Y and Z components of the unit vector in the aircraft-fixed and ground track coordinate systems, respectively; and α, β and γ are the roll, pitch and yaw angles, respectively, in radians, positive when counterclockwise.

Reduced data was accomplished with the assumption that flight lines took place over flat terrain. Accordingly, the coordinates of the ground intercept of the antenna axis are given by

$$x = d - (h / Q_3) Q_1$$

$$y = - (h / Q_3) Q_2$$

where x and y are distances down and cross track of the ground intercept, and d and h are the distance down track and altitude of the aircraft.

The set of triplets (T,x,y) comprise the final output of data processing. (T denotes brightness temperature.) This information, a table of ground locations and corresponding radiometric temperatures, is written on magnetic tape and also printed for permanent hard copy.

Establishment of a Common Origin of Time

The absolute reference for time is the aircraft clock. To relate a measurement of radiometric brightness temperature to the corresponding position and attitude of the airplane, the times of the two data sources must be expressed in the reference timing system. That is, microwave temperature is given as a function of time, and aircraft movement is given as a function of time, and it is required that both functions of time have the same epoch. Also, to calculate the ground intercept of the radiometer antenna axis it is necessary that the times of the beginning and ending of aerial photography and infrared scanning over a flight line be determined in the same timing reference system. The roll, pitch and yaw of the aircraft are given directly in terms of the time of day. Two representative print-outs are illustrated in Tables 7 and 8.

The first entry, which is:

TW = 06110030104

is the thumbwheel setting, mentioned earlier, and is a record of data, line number and other identifying information. The

Tw = 6 1 1 0 0 3 0 1 0 0 4

TIME = 04202

	1	2	3	4	5	6	7	8	9	10
1	421	717	0	157	1124	983	919	332	555	0
2	430	713	5	171	1155	1004	938	334	574	0
3	415	715	1	156	1139	1012	955	347	615	0
4	419	707	0	155	1121	987	941	335	606	0
5	427	770	4	164	1141	977	924	321	579	0
6	413	763	3	164	1149	1008	940	332	567	0
7	431	745	5	161	1161	1006	946	346	608	0
8	417	751	2	152	1123	992	930	339	612	0
9	424	734	5	160	1120	980	917	328	592	0
10	416	738	3	166	1149	1003	934	317	569	0
11	428	775	4	165	1154	1006	956	343	599	0
12	409	693	4	160	1138	1004	955	342	615	0
13	422	716	4	155	1117	983	922	326	590	0
14	424	753	5	165	1135	992	907	323	574	0
15	417	742	4	167	1142	1002	930	335	596	0
16	433	710	5	159	1133	996	944	343	617	0
17	422	753	1	156	1115	986	917	337	600	0
18	424	743	4	154	1137	976	895	319	580	0
19	435	743	4	165	1153	1005	927	336	572	0
20	433	695	3	161	1154	1004	932	345	613	0
21	418	734	2	155	1130	994	924	345	612	0
22	421	731	3	159	1123	984	916	327	594	0
23	424	722	3	167	1151	1003	929	318	573	0
24	417	750	4	166	1152	1008	955	342	599	0

INCREDATA DIGITAL TAPE PRINT-OUT

TABLE 7

TW = 0 6 1 1 0 0 3 0 1 0 0 4

TIME = 64278

	1	2	3	4	5	6	7	8	9	10
1	413	730	4	157	1134	992	911	328	592	0
2	428	709	7	161	1149	1017	919	325	579	0
3	406	685	4	161	1159	1016	962	341	604	0
4	411	699	3	153	1136	998	935	333	612	0
5	429	731	6	162	1140	1001	921	323	585	0
6	415	719	3	167	1160	1012	952	329	592	0
7	398	760	3	157	1141	1005	959	346	609	0
8	426	732	2	155	1126	997	899	319	590	0
9	421	732	6	166	1143	1019	932	331	576	0
10	409	736	3	160	1142	1018	940	341	604	0
11	418	731	1	158	1127	984	913	332	594	0
12	424	768	5	163	1144	1010	917	324	573	0
13	408	721	3	159	1159	1034	916	342	612	0
14	413	717	2	157	1117	999	910	333	606	0
15	432	748	5	163	1148	1016	903	320	583	0
16	406	675	5	164	1161	1022	953	339	597	0
17	426	687	3	150	1137	1009	928	340	613	0
18	425	716	5	161	1145	993	906	327	573	0
19	41	723	5	165	1160	1034	948	334	594	0
20	407	682	4	157	1139	1007	934	340	621	0
21	419	695	6	151	1129	995	912	324	584	0
22	415	751	5	165	1162	1026	931	334	591	0
23	403	675	4	157	1140	1016	938	346	611	0
24	419	720	3	151	1125	1002	912	323	589	0

0006010100000100020000040000000000000000

CONTROL--TW= 0006010100000100020000040000000000000000 DT= -0-0-0 H.M.S. OR

INPUT TW (OCTAL)	INPUT TIME H.M.S.	SECONDS	
	233726	85046	0006010

INCREDATA DIGITAL TAPE PRINT-OUT

TABLE 8

second entry in the tables is a time, e.g., in Table 7, the entry

TIME = 84202

is the aircraft clock time, that is, time of day (in seconds). The remaining entries relate to aircraft motion.

This same information was simultaneously recorded on the serial digital channel of the 14-track analog tape. Figure 28 illustrates a strip chart recording of this channel, along with a recording of the audio channel.*

The serial digital channel appears as broken ribbons of inked paper. Point A is the beginning of one bar. The reason the graph immediately to the right of A is a solid bar is that the data on the tape consists of zeros and ones, since original Incredata data is binary. The zeros and ones are so closely packed that the chart recording pen-line width appears to produce an unbroken bar.

At point A all systems are in a steady state. The numbers in Table 7 are the values (in decimal notation) of the bar starting at Point A. Therefore, the time of Table 7 is the time at Point A.

The audio channel, recorded at the same time as the serial digital channel, and is in synchronization with the serial digital track. Counting the bars on the chart recording of the serial digital channel is one-to-one with counting tables in the printout of the Incredata tape. Thus, the time of day of Point C is readily established, from which the time of the end of valid data, Point D, can be measured.

At the times of insertion of the 400 Hz pulses on the audio channel, some of this energy is diverted to the infrared scanner and light flashes, exposing small dots on the edge of the scanner film. This establishes a time-tie between all systems.

The numbers representing microwave temperatures are assigned reference times in the following way:

When the analog-to-digital conversion takes place the radiometer channel is connected to one pen of the Clevite chart

---

* A reproduction of an actual strip chart recording is not shown, because noise would complicate this explanation.

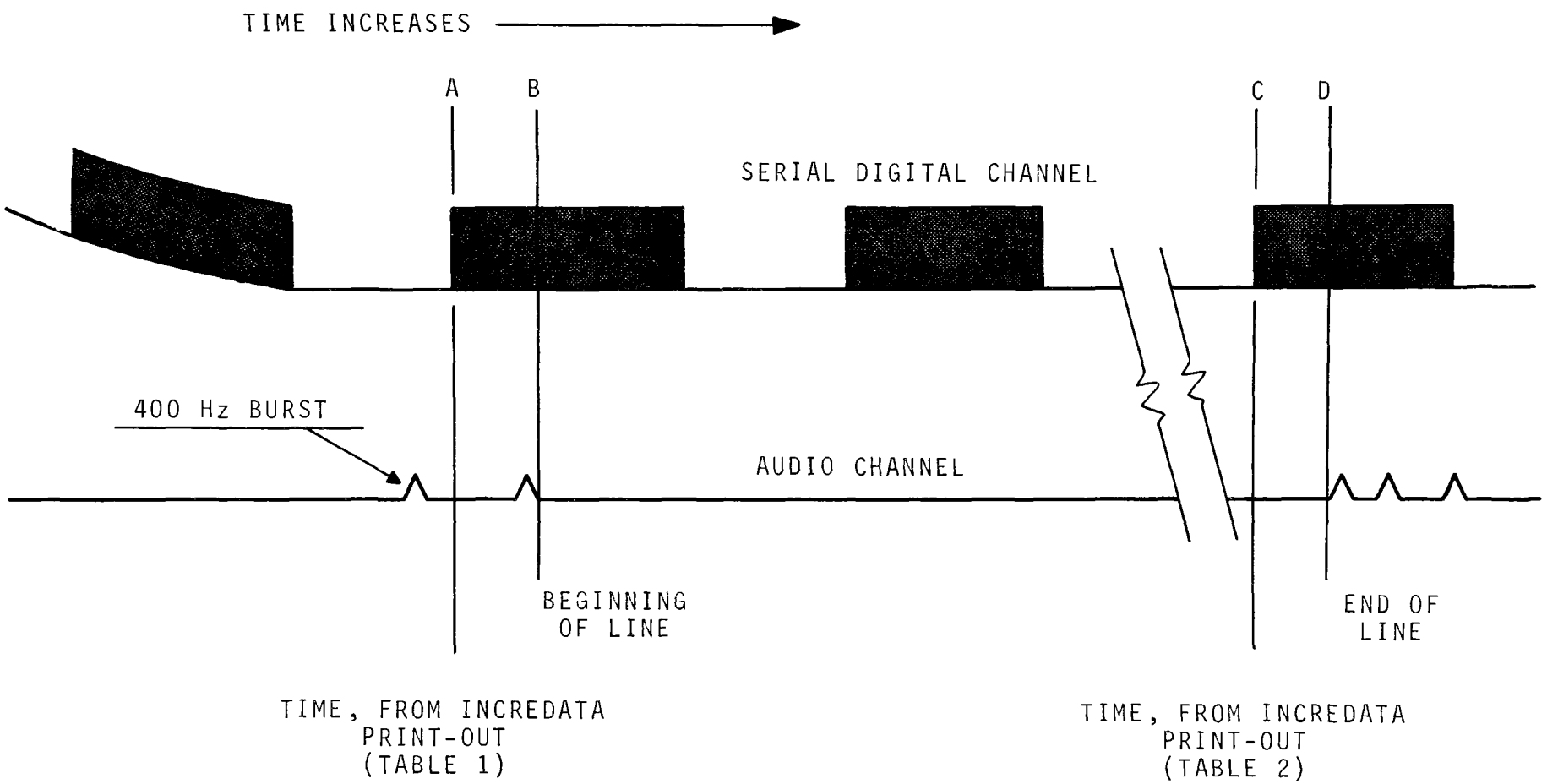

Figure 28 Strip Chart Recording of Serial Digital and Audio Channels

recorder and the digital instrumentation is connected to the other pen. The Ampex machine is turned on in play-back mode and the chart recorder is turned on and one pen begins plotting the random voltages at the beginning of the tape. Then the analog-to-digital coverter is turned on, and the second chart recorder pen changes from drawing a line at zero volts to drawing a line at some non-zero voltage. This chart, showing voltages from the radiometer tape along with the start of analog-to-digital conversion is the key to determining the time of day corresponding to word number one written on a computer tape.*

Figure 29 is a schematic of three strip chart graphs. Point A represents the beginning digitizing. Point B represents the time when the tape recorder aboard the aircraft began recording outputs from the radiometer. Points E and G are the beginning and end of used data.

Spikes on the data as at points D, E and G occur at the ends of one or more of the 400 Hz bursts. These are "wild points" in the digital version and are used to corroborate the correlation between word sound on the digital tape and time on the analog tape. Times during radiometric "events", such as at Point F, are readily found in the digital print-out.

Brightness Temperatures

The fourteen-track analog tape has three channels assigned to microwave radiometer data recording, an audio channel, a serial digital channel, and the radiometer (video) channel. The audio track records the flight log information as spoken by the pilot. The serial digital channel records the Incredata output at the same time the Incredata tape records it--identical information, but the fourteen-track analog tape records the data in serial mode on seven-tracks. Play-back with strip-chart plotting of the serial digital channel and the audio channel simultaneously utilized with the computer print-out of the Incredata digital tape yields the tie between the time of day and the 400 Hz pulses on the audio tape and on the infrared film.

The radiometer channel records a continuously varying voltage proportional to the brightness temperature at the antenna. Plotting this channel and the audio channel at the same time

---

* The word "word" is used in its computer context. For example, "The CDC 6600 has a 60-bit word length."

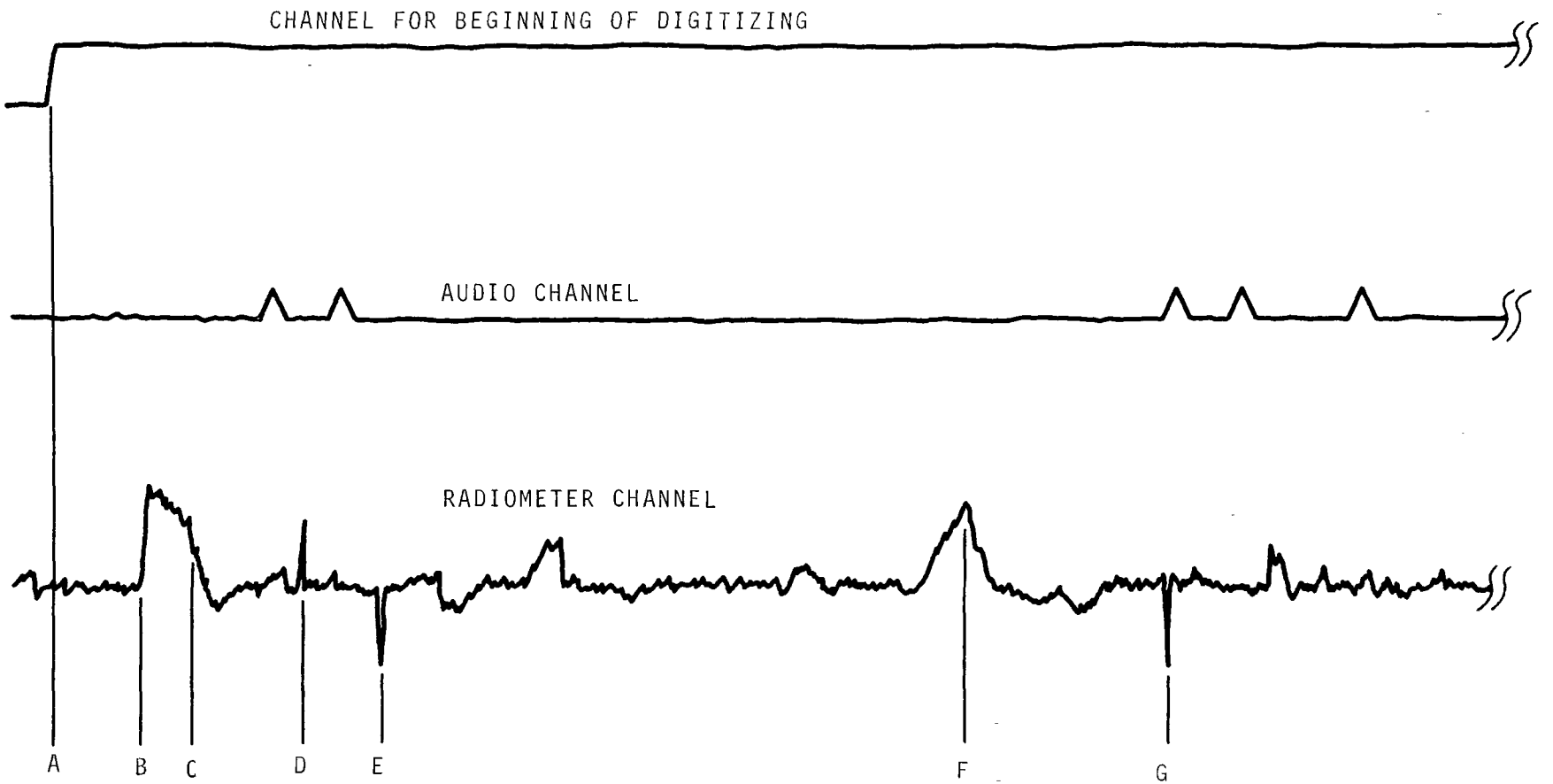

Figure 29 Strip Chart Recording Used For Timing

shows the time-correspondence between the two channels, in particular, the beginning of radiometer data relative to the 400 Hz pulses.

The analog to digital process is performed with a Preston 1400 converter connected with an IBM System 360, Mod 44 computer, and results in an IBM nine-track digital computer tape with record lengths of 512 words.

At this state in the procedure, two digital computer compatible magnetic tapes have been prepared, one containing a history of aircraft attitudes and one containing digital counts proportional to radiometric temperatures.

Data Processing

There are two magnetic tape data sets utilized by the computer, one of aircraft roll, pitch and heading versus time of day, and one of brightness temperature in digital counts versus time of day. The first step in datj processing is to produce a third tape for each flight line containing aircraft position versus brightness temperature in degrees Kelvin.

Input to the computer program which writes the new tapes consists of the following quantities:

- number of files and records from the beginning of the temperature tape to the second 400 Hz burst word
- along-line speed of the aircraft, derived from the doppler system and checked by imagery measurements
- number of words of original data averaged to make one output value
- flag to employ the option to compute the standard deviations of output values
- flag to employ the option to filter the output values
- filter length, if output values are to be filtered
- flag to employ the option to print the output values, if desired

- flag to employ the option to reverse the order of the input data, if required
- site number and line number
- factor to convert digital counts to degrees Kelvin
- correction to zeroset of radiometer, if required
- effective realtime sampling rate used in the analog-to-digital process
- time of the first data point

The data is compressed by averaging a number of input temperatures and considering the average to be an improved temperature located at the midpoint of the number of values averaged. Data compression is also employed to reduce the number of points which must be processed. The corresponding ground distances between temperatures are of the order of magnitude of one foot and one-tenth feet, respectively.

The algorithm for converting digital counts to brightness temperatures is derived in the following way: The Prescott 1400 Analog-to-Digital Converter is adjusted to that five volts from the analog tape would fill its 13-digit register with 1's. This means that

$$0 \text{ volts} = 0 = 0^{o}K$$

$$5 \text{ volts} = 2^{13} - 1 - 8191 = 500^{o}K$$

since the radiometer circuit is calibrated at 1 volt equals $100^{o}K$. Therefore

$$1 \text{ count} = 500 / 8191 = .06104261^{o}K$$

Flight lines processed with this equation yield brightness temperatures with reasonable values for the thermometric ground temperatures measured by ground crews.

Profiles which are plotted on an X-Y plotter provide a graph of temperature versus distance down line. The distance down line is the perpendicular projection of the actual ground intercept on the flight line.

1 Accession Number	2 Subject Field & Group	SELECTED WATER RESOURCES ABSTRACTS INPUT TRANSACTION FORM
W		

5 Organization

RESOURCES TECHNOLOGY CORPORATION

6 Title

Fluid Product Pipeline Leak Detection from Airborne Platforms

10 Author(s)

Joseph Kennedy

16 Project Designation

Program #16020 FQT / 12/70

21 Note

22 Citation

December 1970, Final Report, Demonstration Grant 16020 FQT, 89 pp

23 Descriptors (Starred First)

Microwave Radiometry, Remote Sensing, Infra-red Imagery.

Pipeline Leak

25 Identifiers (Starred First)

Pipeline Leak

27 Abstract

A project to demonstrate the applicability of microwave radiometry to pipe detection of leaks in pipelines. The demonstration involved flights over three different pipeline sections containing known leaks determination of the apparent microwave temperature, microwave polarization contrast and taking of infrared imagery was carried out and correlated with ground data.

It was found that the apparent microwave (13.7 GHz) temperature increased significantly at the site of a leak. Also, the polarization contrast decreased and the infrared imagery showed a warm area surrounded by a cool halo. When these three circumstances occurred together a leak was positively identified.

Abstractor Louis G. Swaby | Institution Environmental Protection Agency

WR 102 (REV JULY 1969)
WRSIC

SEND, WITH COPY OF DOCUMENT, TO: WATER RESOURCES SCIENTIFIC INFORMATION CENTER
U.S. DEPARTMENT OF THE INTERIOR
WASHINGTON, D. C. 20240

☆U.S. GOVERNMENT PRINTING OFFICE: 1972 484-483/61 1-3